Journal of Medicinal Chemistry

Article

Highly Effective Dual-Function Near-Infrared (NIR) Photosensitizer for Fluorescence Imaging and Photodynamic Therapy (PDT) of Cancer

Nayan Patel, Paula Pera, Penny Joshi, Mykhaylo Dukh, Walter A Tabaczynski, Kevin E. Siters, Mark Kryman, Ravindra R. Cheruku, Farukh Durrani, Joseph R. Missert, Ramona Watson, Tymish Y. Ohulchanskyy, Erin Tracy, Heinz Baumann, and Ravindra K. Pandey

J. Med. Chem., **Just Accepted Manuscript** • DOI: 10.1021/acs.jmedchem.6b00890 • Publication Date (Web): 17 Oct 2016

Just Accepted

ACS Publications

Journal of Medicinal Chemistry is published by the American Chemical Society. 1155 Sixteenth Street N.W., Washington, DC 20036

Highly Effective Dual-Function Near-Infrared (NIR) Photosensitizer for Fluorescence Imaging and Photodynamic Therapy (PDT) of Cancer

Nayan Patel,[1,2] Paula Pera,[1] Penny Joshi,[1] Mykhaylo Dukh,[1] Walter A. Tabaczynski,[1] Kevin Siters,[3] Mark Kryman,[3] Ravindra R. Cheruku,[1] Farukh Durrani,[1] Joseph R. Missert,[1] Ramona Watson,[1] Tymish Y. Ohulchanskyy,[4,5] Erin Tracy,[6] Heinz Baumann[6] and Ravindra K Pandey[1,2,3*]

[1]Photodynamic Therapy Center, Department of Cell Stress Biology, [2]Department of Pharmacology, [6]Department of Molecular Biology, Roswell Park Cancer Institute, Buffalo, NY 14263, [3]Photolitec, LLC, 73 High Street, Buffalo, NY 14203 and College of Optoelectronic Engineering, Shenzhen University, Shenzhen, Guangdong, China, 518060 and [5]Institute of Lasers, Photonics and Biophotonics, University of Buffalo, Buffalo, NY 14260

ABSTRACT

We report herein, the synthesis and biological efficacy of near-infrared (NIR), bacteriochlorin analogs: 3-(1'-butyloxy)ethyl-3-deacetyl-bacteriopurpurin-18-N-butylimide methyl ester (**3**) and the corresponding carboxylic acid **10**. In *in vitro* assays, compared to its methyl ester analog **3**, the corresponding carboxylic acid derivative **10** showed higher photosensitizing efficacy. However, due to drastically different pharmacokinetics *in vivo*, the PS **3** (HPLC purity > 99%) showed higher tumor uptake and long-term tumor cure than **10** (HPLC purity > 96.5%) in BALB/c mice bearing Colon26 tumors. Isomerically pure *R*- and *S*- isomers of **3** (**3a** and **3b**, purity by HPLC >99%) under similar treatment parameters showed identical efficacy *in vitro and in vivo*. In addition, photosensitizer (PS) **3** showed limited skin phototoxicity, and provides an additional advantage over the clinically approved chemically complex hematoporphyrin derivative as well as other porphyrin-based PDT agents, which makes **3** a promising dual-function agent for fluorescence-guided surgery with an option of phototherapy of cancer.

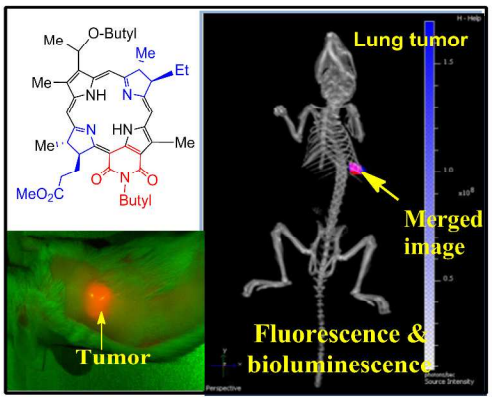

INTRODUCTION

Porphyrin-based compounds, especially the chlorins and bacteriochlorins in which one or two pyrrole units (diagonal to each other) are reduced respectively have shown enormous interest for NIR fluorescence imaging and photodynamic therapy (PDT) of cancer[1-3]. These tetrapyrrolic compounds can be synthesized either via a multi-step synthesis or by partial modification of naturally occurring chlorophyll-a and bacteriochlorophyll-a, which can be isolated from Spirulina algae and *Rb. sphaeroides* respectively[4]. We and others have previously reported a large number of effective PDT agents derived from chlorophyll-a and bacteriochlorophyll-a[5]. Even though some of these compounds are highly fluorescent and quite effective both *in vitro* and *in vivo,* but due to limited Stokes shift in the NIR, these compounds are not ideal candidates for fluorescence imaging or fluorescence-guided PDT of large and deeply seated tumors[6,7]. The optical properties of a tissue affect both diagnostic and therapeutic applications of light. The ability of an appropriate wavelength of light to penetrate tissue with less scattering, interact the tumor–avid photosensitizer (PS), then emit from the tissue for detection is essential to diagnostic applications[8]. The irradiation of a PS in tissue, excite the PS the first excited singlet state. After inter system crossing (ISC), the PS excited triplet state can undergo two kinds of reactions. First, it can react with the substrate to form radical species, which on further reaction with oxygen to yield oxygenated products (type I reaction). It can also undergo a photophysical process known as Type II reaction, which converts the triplet molecular oxygen present in tumor to highly reactive singlet oxygen, believed to be a key cytotoxic agent for the destruction of tumor cells by PDT[9]. However, the depth of light penetration also depends on the tumor-type. Therefore, it is of utmost importance to define the optical properties of a tissue in designing the devices for optimization of imaging and therapeutic potential of a photosensitizer/imaging agent.[9]

Among the bacteriochlorins investigated so far, a water soluble palladium-bacteriopheophorbide photosensitizer is currently in Phase III trials in Europe as a vascular

targeted prostate cancer treatment[10]. The Pd-bacteriopheophorbide's NIR absorption (763 nm) and water solubility make it an excellent PDT agent. However, it has a very short half-life in the body. It is classified as a vascular targeted PDT agent and since it is ineffectively taken up by tumor cells at extravascular sites, it has no target selectivity. The presence of palladium as a central metal in Pd-bacteriopheophorbide-a increases its singlet oxygen yield (heavy atom effect)[11], which enhances PDT, but it has limited fluorescence quantum yield, which diminishes its utility as dual-function (imaging and therapy) agent.

We have been investigating the use of certain tumor-avid PS as dual-imaging (fluorescence/PET[12-14], fluorescence/SPECT[15] and fluorescence/MRI)[16,17] agent(s). The main objective has been to develop a single molecule or a nanoplatform for imaging with an option of directing surgery and photodynamic therapy. Surgery is the prime and essential component in the curative treatment for the majority of cancer patients. Therefore, NIR fluorescence-guided surgery in combination with PDT could be extremely useful in treating various cancer types. For developing a NIR fluorescence agent it is of the utmost importance that the compound exhibits a significant Stokes shift at near-infrared region with high fluorescence. The agent should be retained by the tumor for a sufficient length of time for detection and photoreaction. This fluorescence guided resection (FGR) has the compelling ability to allow the surgeon a precise location of the tumor bed which can improve tumor resection and tumor control, without any injury to normal tissue[18].

Herein, we report the synthesis, characterization, photophysical properties, tumor-imaging, therapeutic potential of NIR bacteriochlorin **3**, and the corresponding stereoisomers (*R-& S-)* as potential candidates for tumor-imaging and PDT. The advantages of PS **3,** over purified form of , 3-(1'-hexyloxy)ethyl-3-devinylpyropheophorbide-a (HPPH, **1**) and purpurinimide **2** are also presented. The structures of these photosensitizers are shown in Figure 1.

RESULTS AND DISUSSION

Chemistry

For developing tumor-specific PDT agents both active and passive approaches have been investigated by us and others, which resulted in some interesting findings. However most of the PDT agents which are currently at various stages of preclinical and clinical trials were developed by following the structure-activity relationship (SAR) and quantitative structure activity relationship (QSAR) studies[19-21]. The Roswell Park Cancer Research (RPCI) group was successful in identifying **1** with a long wavelength absorption at λ_{max} 665 nm *(in vivo)* as the most effective candidate from a homologous series of alkyl ether analogs of pyropheophorbide-a,[21-23] and will be undergoing Phase II clinical trials of head & neck cancer[24].

For developing photosensitizers with longer wavelength absorption, the long wavelength absorption of **1** was red-shifted by replacing the five member isocyclic ring with a six member N-alkyl imide ring system, and the resulting purpurinimide class of compound exhibited a NIR absorption at 700 nm[25]. Among a series of alkyl-ether analogs evaluated for PDT efficacy, the N-butyl and O-butyl purpurinimide **2** was selected due to its excellent biological efficacy and ease of synthesis.

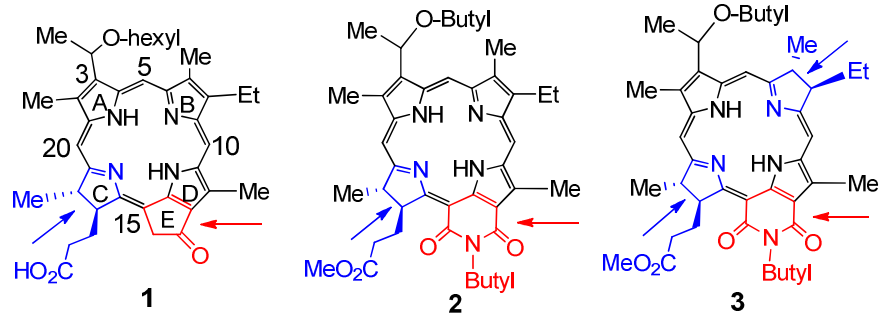

1 **Pyropheophorbide** (HPPH or Photochlor)

2 **Purpurinimide** (PS-277)

3 **Bacteriopurpurinimide** (Photobac)

Figure 1: Photosensitizers derived from chlorophyll-a and bacteriochorophyll-a bearing a five member isocyclic or a six member imide ring system. Arrows denote the reduced pyrrole ring(s).

To further understand the impact of structural correlation of the chlorin *vs.* bacteriochlorin

system in biological efficacy, we retained all the structural parameters of purpurinimide, but replaced the ring 'B' with a reduced pyrrole unit, which produced a significant red shift (82 nm)

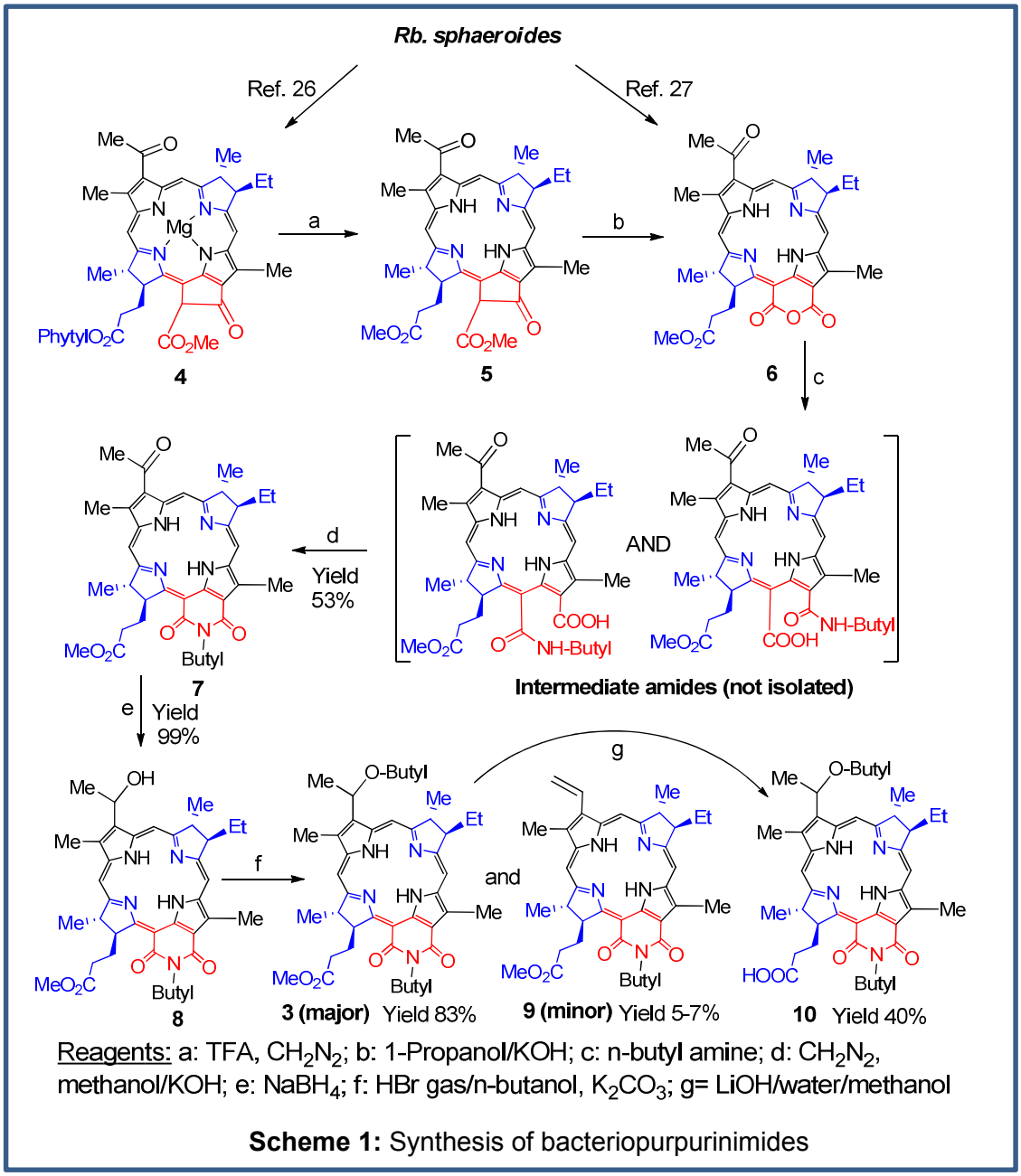

Scheme 1: Synthesis of bacteriopurpurinimides

in its long wavelength absorption (λ_{max} 782 nm). The desired bacteriopurpurinimides as methyl ester **3** (3-(1'-butyloxy)ethyl-3-deacetyl-bacteriopurpurin-18-N-butylimide methyl ester; Photobac) and the corresponding carboxylic acid **10**, were prepared by following the reaction sequences shown in **Scheme 1**

In our approach, bacteriochlorophyll-a **4** was extracted from *Rb. sphaeroides*, which on treating with trifluoroacetic acid (TFA) and then with CH_2N_2 (diazomethane) afforded methyl bacteriopheophorbide-a **5**[26]**.** The five member isocyclic ring present in **5** was converted into a six member anhydride ring system **6** by following the methodology reported for the preparation of bacteriopurpurin-18 methyl ester[27]. Methyl bacteriopurpurinimide **6** on reacting with n-butyl amine gave an isomeric mixture of the intermediate amides, which were not isolated and immediately treated with methanolic KOH to afford the 3-acetyl-bacteriochlorin-n-butylimide **7** in 75 % yield. Due to a significant difference in long wavelength absorptions between the anhydride *vs.* imide ring systems, as well as the intermediate amides, the conversion of **6** to **7** can be monitored by UV-vis spectroscopy (**Figure 2**).

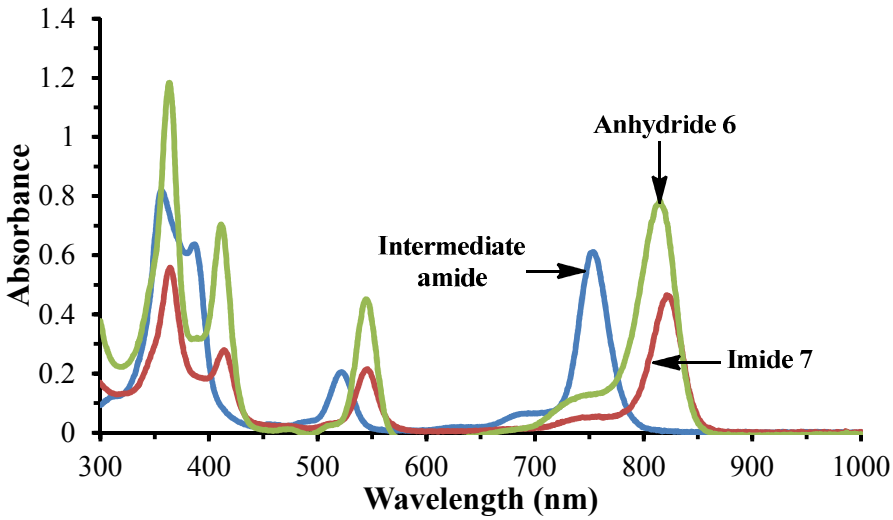

Figure 2: Absorption spectra of bacteriochlorins containing an anhydride (**6**), intermediate amide or an imide (**7**) ring system in methanol (not in equimolar concentrations).

The 3-(1'-hydroxy)ethyl analog **8** obtained on reacting **7** with sodium borohydride was reacted with HBr gas at room temperature. The intermediate bromo- derivative was not isolated but immediately reacted with n-butanol in presence of anhydrous potassium carbonate. The desired butyl ether analog **3** was obtained as a major product (83% yield) along with 3-vinyl-N-butylpurpurinimide **9** as a minor product in 5-10 % yield. In a separate approach, we followed a

similar methodology except the starting material **6** was directly isolated from *Rb. sphaerodes* in almost the same yield. The second approach is advantageous as it eliminated the initial two steps of the original synthetic procedure.[27]

The structures of the intermediates and the final products were confirmed by NMR (^{1}H and ^{13}C-), high resolution mass (HRMS) and/or elemental analyses. The purity of the final product as methyl ester and carboxylic acid analogs was also confirmed by HPLC analysis. Due to the presence of a chiral center at position-3(1') of bacteriochlorin **3**, it was isolated as a mixture of *R*- & *S*- stereoisomers. To compare the *in vivo* and *in vitro* biological efficacy of the individual isomers, both isomers were separated by HPLC using a Waters Symmetry preparative column and methanol as mobile phase (**Figure 3**). The purity of both the possible isomers was confirmed by NMR and mass spectrometry analyses. However, no difference in biological efficacy of individual isomers was observed. Therefore, the stereochemistry *(R- or S-)* of individual isomers at position 3(1') was not established. The isomer with retention time 15.3 min was coded as **3a** and the other eluted at 16.9 min was coded as **3b**.

Proton NMR spectral assignment was aided by information obtained from cross peaks observed in 2-D NMR spectra (Supplemental material, **Figure S19**) acquired for compound **8**. These spectra include homonuclear 2D ^{1}H COSY, NOESY, and TOCSY, as well as 2D heteronuclear ^{1}H-^{13}C HSQC. NOESY spectra were especially useful in making the *meso* proton assignments. NOESY cross peaks for compound **8** indicate through-space interactions between the meso proton at 8.81 ppm and the 3^{1}-H (6.21 ppm) and 3^{1}-CH_3 (2.05 ppm) protons. These cross peaks identified this meso proton as 5-H. Additional cross peaks, between 5-H and the 7-H (4.20 ppm) and 7-CH_3 (1.79 ppm) protons, further substantiated this assignment. The assignment of the 10-H *meso* proton was made in a similar way. Here, the NOESY spectrum showed that the meso proton at 8.61 ppm interacts with the 12-CH_3 (3.62 ppm), 8-H (4.01 ppm), 8-CH_2CH$_3$ (2.03 and 2.33 ppm), and 8-CH_2CH_3 (1.11 ppm) protons. Likewise, 20-H was assigned using correlations observed between the *meso* proton at 8.33 ppm and the 2-CH_3

(3.27 ppm), 18-H (4.19 ppm) and 18-CH_3 (1.68 ppm) protons. Further interpretation of the 2D spectra allowed assignment of the remainder of the protons of **8**. The ^{1}H spectral assignment of **8** was useful in interpreting and assigning the 1H spectra of **3**, **7**, **9**, and **10**, which have similar structures.

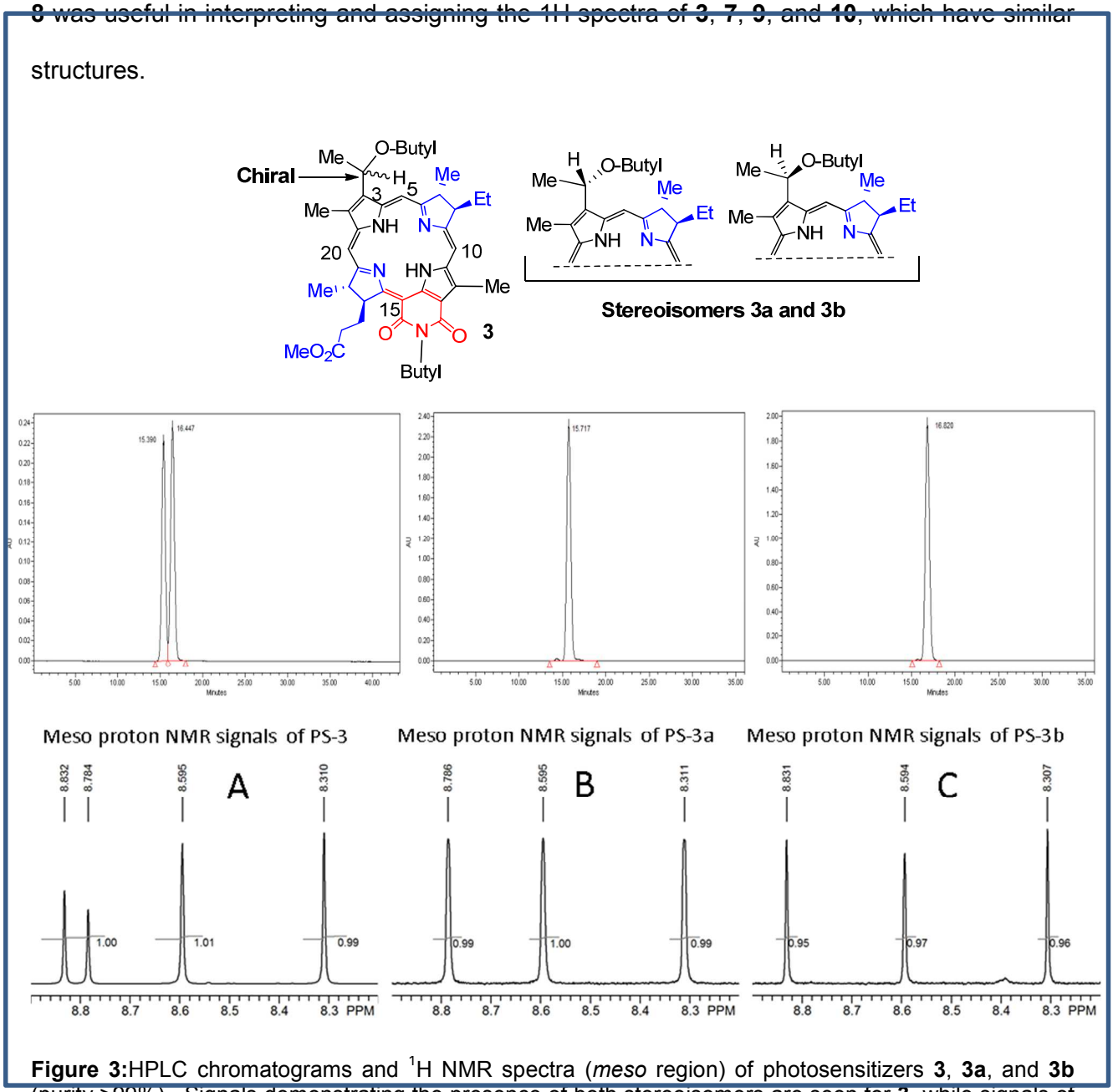

Figure 3:HPLC chromatograms and ^{1}H NMR spectra (*meso* region) of photosensitizers **3**, **3a**, and **3b** (purity >99%). Signals demonstrating the presence of both stereoisomers are seen for **3**, while signals of the individual isomers are observed for **3a** and **3b**. Two distinct 5-H NMR resonances (*meso* proton at position 5)are observed at ~8.8 ppm for the mixture of the two isomers (A), while each of the isolated stereoisomers shows only one 5-H peak (B and C).

Compound **3** is a mixture of two unresolved stereoisomers. These two forms are possible because of chirality at C3[1]. The influence of this stereoisomerism is nicely illustrated

by the *meso* region of the proton NMR spectrum of **3**, where two distinct signals (at 8.832 ppm and 8.784 ppm; **Figure 3A**) were observed for the 5-H proton. In contrast, each of the two isolated stereoisomers (**3a** and **3b,** HPLC purity >99%) showed only a single resonance for 5-H (**Figure 3B** and **3C**), demonstrating a complete resolution of the *R*- and *S*- forms. Chemical shifts of the 5-H signals of the isolated forms closely match those of the pair of 5-H signals observed for the mixture. Unlike 5-H, the 10-H and 20-H *meso* protons did not show a significant difference in chemical shifts observed for the two stereoisomers. These protons are further removed from the chiral center and were observed as singlets in **3** (**Figure 3A**), showing no peak doubling due to stereoisomerism.

For evaluating the biological efficacy of methyl ester vs. the corresponding carboxylic acid analog, **3** was reacted with aqueous lithium hydroxide and corresponding carboxylic analog **10** was isolated in 40% yield. The structure was confirmed by NMR (^{1}H, ^{13}C-), HRMS and purity was confirmed by HPLC [Column: Waters C18 Symmetry (4.6 x 150 mm, 5 μ particle size), mobile phase 0.5% (v/v) acetic acid in methanol; flow rate: 1.0 ml/min), retention times: 9.39 and 10.00 minutes], see Figure S21, Supplemental Information.

Photophysical properties

Photophysical properties for both bacteriopurpurinimide analogs **3** (-methyl ester) and **10** (-carboxylic acid) were examined in methanol and both analogs showed identical absorbance and fluorescence characteristics with similar extinction coefficients values. **Figure 4** displays the absorbance and fluorescence spectra of bacteriopurpurinimide **3** in methanol. Structurally, the only difference between **3** and **10** is that compound **3** contains a methyl ester functionality at position-17[2] whereas compound **10** has a carboxylic acid functionality at the same position. Since neither of these functional groups alters the electronic structures of the aromatic system of the PS, these compounds are not expected to have a significant difference in their optical properties. Both photosensitizers exhibit wavelength absorption at 782 nm (in methanol) and a broad fluorescence emission is observed at 830nm. The fluorescence band is quite broad with

peaks at 850 and 920 nm with no overlap with the absorption band beyond 830 nm. Such an inherent characteristic provides an opportunity to excite the photosensitizer at its longest absorption wavelength and measure the fluorescence > 830 nm. This is a unique characteristic specific to this particular class of Absorption ⟵ ⟶ Fluorescence compounds and was not observed so far with other PDT agents related to chlorins and purpurinimide systems derived from chlorophyll-a.

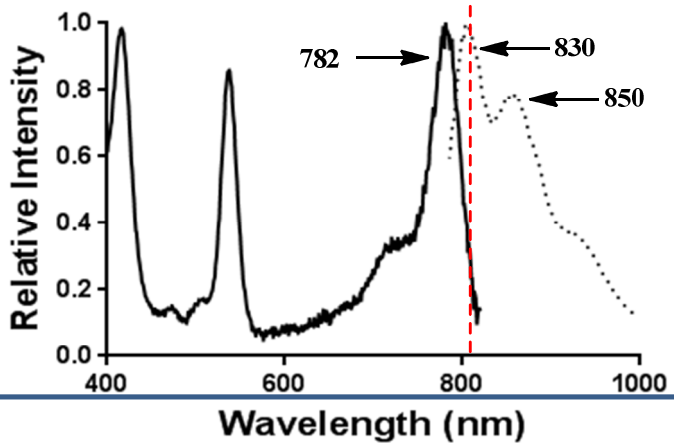

Figure 4: Relative absorption (solid line) and fluorescence (dotted line) spectra of **3** in methanol at 5 μM concentration. However, compound **3** in the presence of BSA (bovine serum albumin) or HSA (human serum albumin) gave a red shift of 5 nm with a broad NIR absorption at 782 nm.

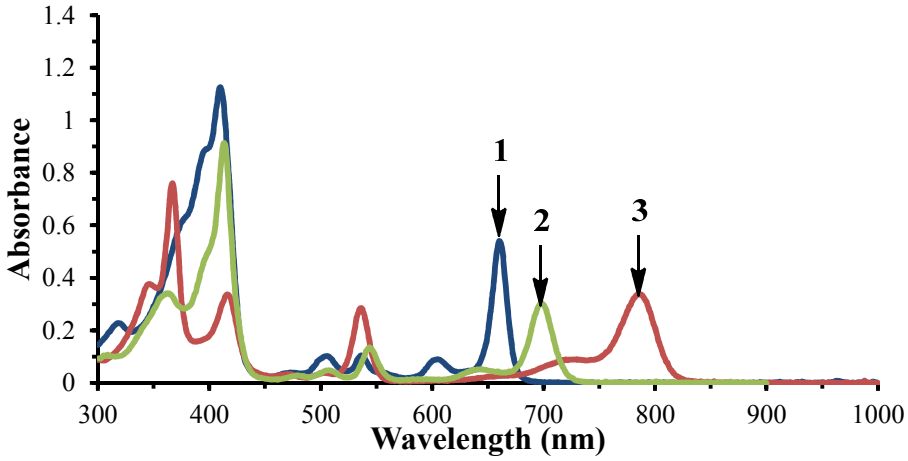

Figure 5: Comparative absorption spectra of HPPH **1** (a chlorin with 5 member fused isocyclic ring), purpurinimide **2** (a chlorin with six member fused imide ring) and bacteriopurpurinimide (**3**), a bacteriochlorin containing a six member fused imide ring, in methanol (not in equimolar concentrations).

We have previously reported a detailed photophysical and electrochemical properties of related bacteriochlorin analogs. The relative singlet oxygen quantam yield was in the range of 0.45-0.48.[28]

***In vitro* cell-uptake, subcellular localization and photosensitizing efficacy of bacterio-purpurinimides 3 and 10:**

To investigate a correlation between cell uptake in *in vitro* photosensitizing activity and PDT efficacy, the photosensitizing efficacy of **3** and its carboxylic acid analog **10** was determined in Colon26 tumor cells by following the standard MTT assay.

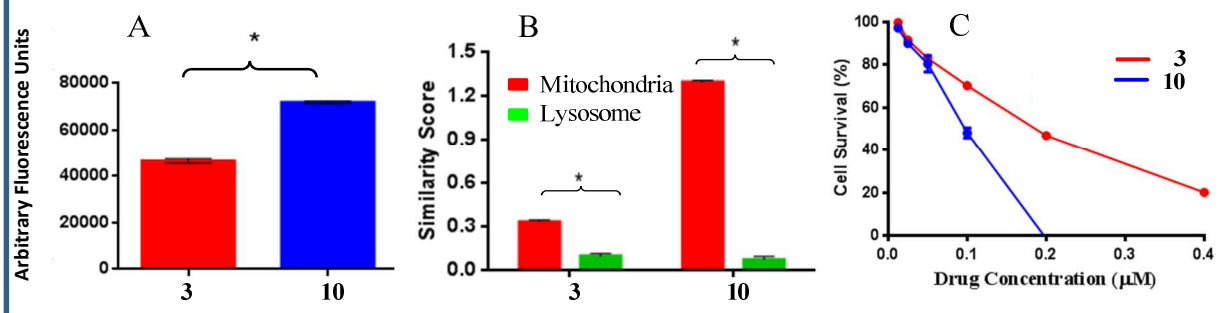

Figure 6: *In vitro* cell-uptake **(A)**, subcellular distribution **(B)**, and photosensitizing efficacy (**C**) of **3** and the carboxylic acid **10**. **(A)** Cell-uptake by flow cytometry, **(B)** subcellular localization in mitochondria (red) and lysosome (green). Distribution was measured in terms of similarity score which is a measure of co-localization with mitochondrial (CMXRos – Ex, 561 nm, Em, 595-660 nm) or lysosome (green Fluoropheres -Ex. 488 nm, imaging window. > 500 nm). **(C)** *In vitro* PDT (A): Colon 26 cells were incubated with various concentrations of the PSs for 24h and then irradiated with light 0.25 J/cm^2 (787 nm) and the cell viability was determined by MTT assay. All 3 experiments were done in triplicate. Error bars represent standard deviation, $p < 0.05$. These compounds did not show any dark toxicity (no light exposure).

The tumor cells were incubated with PS for 24h and uptake was measured by flow cytometry (**Figure 6A**) and the subcellular site of retention was defined by image stream analyses following the standard methodology.[29] Compared to **3** the carboxylic acid **10** showed almost 2-fold higher uptake and enhanced localization in mitochondria (**Figure 6B**). Treatment of Colon26 tumor cells with light at 787 nm at a fluence rate of 0.25J/cm^2, and compound **10** was more effective than **3 (Figure 6C).**

***In vivo* uptake (by fluorescence and ^{14}C-) and comparative PDT efficacy of 3 and the corresponding carboxylic acid 10:**

Based on *in vitro* information, we expected a similar trend regarding *in vivo* tumor uptake and PDT efficacy of **3** and **10**. Both compounds were evaluated in BALB/c mice bearing Colon26 tumors. The tumor-uptake of these compounds at variable time points was determined by fluorescence imaging. In brief, three tumor bearing mice (BALB/c) per group were injected with **3** and **10.** The mice were imaged over the course of 48h (**Figure 7A**). Using the built-in Maestro image analysis software, the fluorescence signal in tumors was quantified at variable time points for both the methyl ester and the carboxylic acid.

Unlike the *in vitro* results, **3** showed a higher level of uptake than the corresponding

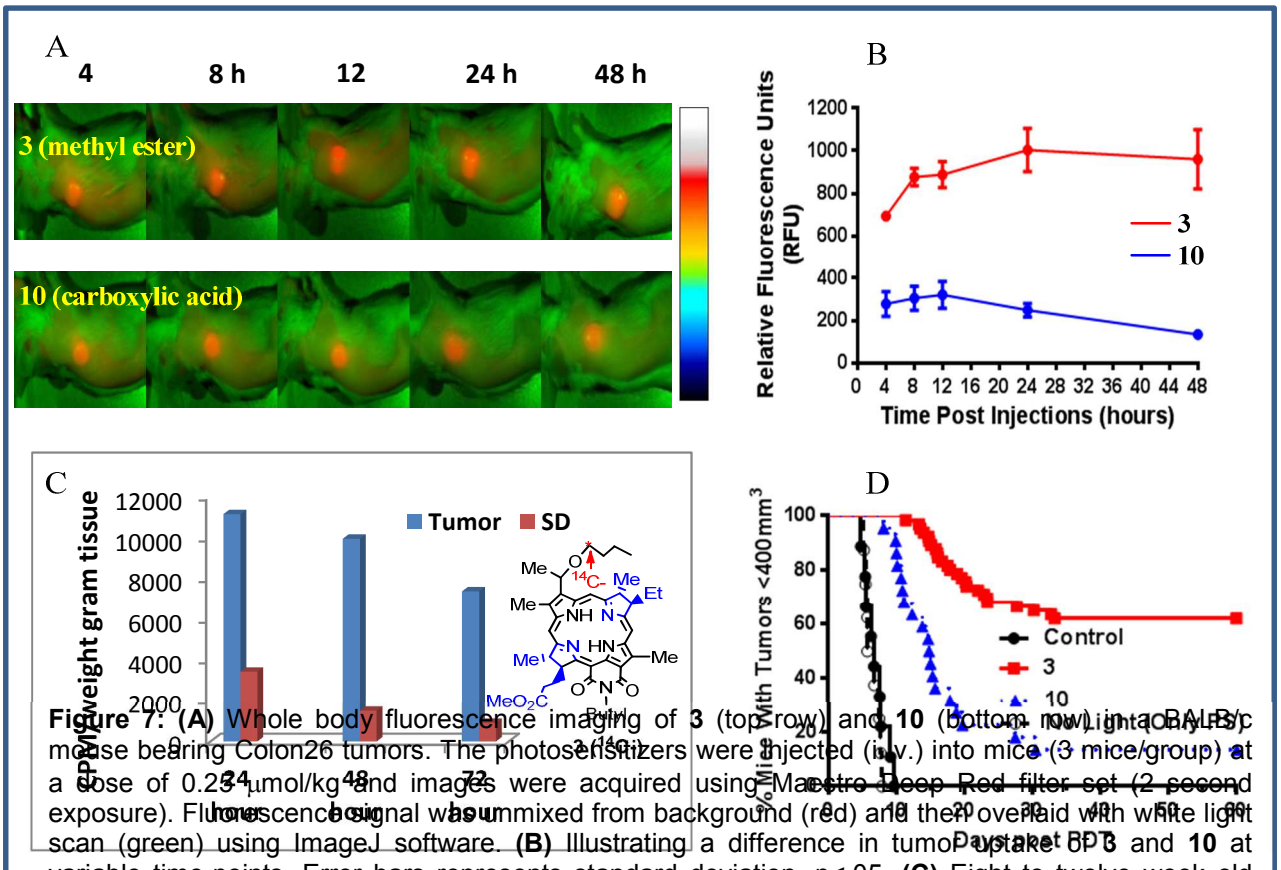

Figure 7: (A) Whole body fluorescence imaging of **3** (top row) and **10** (bottom row) in a BALB/c mouse bearing Colon26 tumors. The photosensitizers were injected (i.v.) into mice (3 mice/group) at a dose of 0.25 µmol/kg and images were acquired using Maestro Deep Red filter set (2 second exposure). Fluorescence signal was unmixed from background (red) and then overlaid with white light scan (green) using ImageJ software. **(B)** Illustrating a difference in tumor uptake of **3** and **10** at variable time-points. Error bars represents standard deviation, p<.05. **(C)** Eight to twelve week old female BALB/c mice implanted with Colon26 tumors, and 1.0 µmole/kg [14]C-labeled **3** (0.1 µCi/mouse) was administered i. v. At 24, 48 and 72 h post-injection, 3 mice/group/time point were euthanized. Tumors and the surrounding muscle were removed, weighed, solubilized and the radioactivity was measured. Results are expressed as the mean cpm/gram tissue ±SD of three mice/time point. Error bars represents standard deviation, p<.05 (*^{14}C- analog was synthesized by following the reaction sequences shown in Scheme 2).* **(D)** *In vivo* tumor response of **3** (red) and **10** (blue) in BALB/C mice implanted with Colon26 tumors. Twenty four hours post injection of PS **3**, 0.25 µmole/kg) mice were treated with laser light at 787 nm at a dose of 135 J/cm^2 and 35 mW/cm^2. Tumor growth was monitored for a period of 60 days post PDT treatment. The PDT response was statistically different from one another (p<0.05 by Mantel-Cox test). SD: Standard deviation. For control experiment only PS 3 (no light) was used at a therapeutic dose.

carboxylic acid **10** at each time point (4, 8, 12, 24 and 48 h post-injection), which starts declining after 24 h post-injection. During the course of imaging, the retention of PS **3**, which was statistically higher than **10** ($p < 0.05$), and the maximum uptake was observed at 24h post-injection **(Figure 7B).** Additionally, there was a significant difference in the tumor-retention between the two PSs. Compound **3** retained in the tumor for an extended time, whereas the maximal uptake of the corresponding carboxylic acid **10** was observed at 4h post-injection. The data suggest a distinct pharmacokinetic property of 3 bearing a methyl ester functionality and its carboxylic acid derivative suggesting the latter having several fold faster clearance. The detailed pharmacokinetic (PK), pharmacodynamics (PD) and toxicity studies of **3** in rats and dogs following the US FDA guidelines are underway.

Fluorescence optical imaging in animals or organs is useful for determining the relative distribution of a fluorophore. The technique is acceptable for comparison of two optically identical fluorophores within the same organ, e. g., tumor *vs.* another tumor. However, it is not reliable to compare two different organs, e. g. accumulation in tumor *vs.* liver. This is due to the difference in the optical properties within different tissues which can interfere with signal detection. For example, dark and dense tissues such as the liver and kidney allow less light to penetrate and reflect compared to lighter tissues such as intestine and muscle. Therefore to truly understand the tissue distribution of **3**, the ^{14}C- analog of **3** (**^{14}C-3**) was synthesized (as a mixture of *R*- and *S*- isomers, **Figure 8**) by following the methodology depicted in **Scheme 2**. Similar to the *in vivo* fluorescence optical imaging, **^{14}C-3** showed maximum tumor uptake at 24-

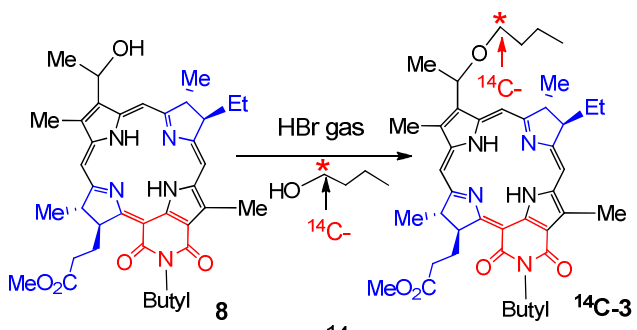

Scheme 2: Preparation of ^{14}C-analog of **3**

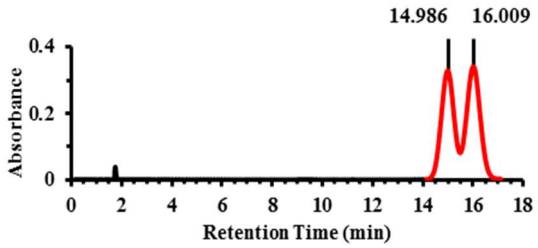

Figure 8: HPLC profile of **^{14}C-3**

48 h post-injection, with no statistical difference (**Figure 7C**).

The *in vivo* accumulation studies indicated that **3** (fluorescence and ^{14}C-) and carboxylic acid **10** (fluorescence only) show optimal accumulation at 24 h and 12 h post-injection respectively (**Figure 7B**). Therefore, to correlate the tumor-uptake data with PDT efficacy, both compounds were evaluated in BALB/c mice bearing Colon26 tumors, using the drug doses ranging from 0.25 to 0.5 μmol/kg. For **3**, the tumors were exposed to 787 nm light (135 J/cm^2, 75 mW/cm^2) at 24 h post-injection and for **10** at 12h post-injection using the same light fluence and fluence rate . The regrowth of the treated tumors was monitored daily. In the initial study, 5 mice/group were used and **3** at a dose of 0.25 μmol/kg, gave 80% complete response (4/5 mice) at day 60 post-treatment. Under similar treatment parameters, the corresponding carboxylic acid **10** showed limited PDT efficacy. Both compounds using identical conditions were again evaluated in larger groups of mice. The combined results obtained from treating 66 tumor bearing mice with **3,** and 22 mice with PS **10** are summarized in **Figure 7D**. Combined data from *in vivo* PDT experiments demonstrated a correlation with distinctive pharmacokinetics of the PS, and a higher PDT efficacy was observed for **3** than the corresponding carboxylic acid derivative **10**. In separate experiments, BALB/c mice bearing Colon26 tumors were also treated with light at 12 and 48 h post injection of the PSs, resulting a lower PDT response (long-term cure).

Cellular uptake, subcellular localization and *in vitro* PDT efficacy of stereoisomers 3a and 3b:

Structurally, compound **3** exists as a mixture of two stereoisomers and, as a part of pre-clinical testing required by the US FDA, the individual isomers were separated by HPLC, and characterized by NMR (^{1}H & ^{13}C-) (see the experimental part and supplemental information) before evaluating their *in vitro* and *in vivo* uptake and biological efficacy. The intracellular localization of epimeric mixture **3** and the related isomers **3a** (retention time: 15.39) and **3b**

(retention time: 16.44) were subjected to similar *in vitro* experiments in Colon26 tumor cells, as discussed previously, for compounds **3** and **10**. Results summarized in **Figure 9A** showed no difference in the cellular uptake of the isomeric mixture and the individual isomers. Imaging analysis **(Figure 9B)** indicated some difference in subcellular localization of the individual isomers, especially isomer **3b** with an apparent higher accumulation in mitochondria than the

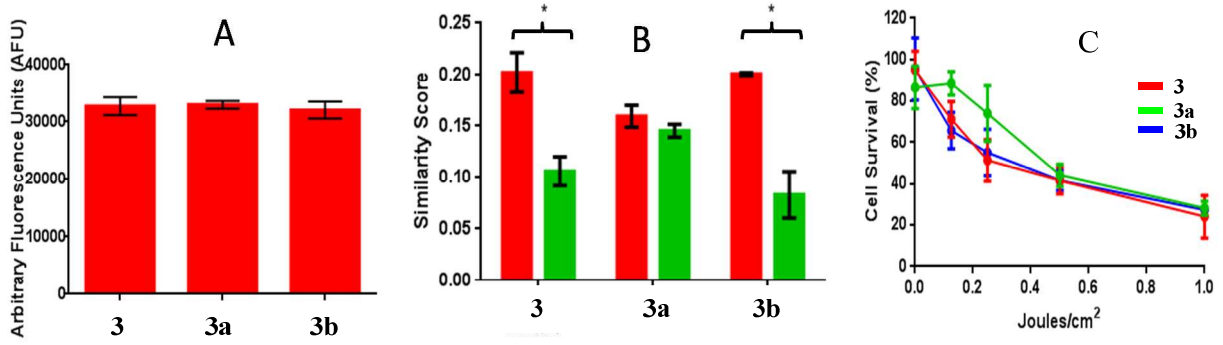

Figure 9: *In vitro* uptake and subcellular distribution of **3** and isomers (**3a**, eluted first in HPLC, and **3b,** eluted later). Colon 26 cells were incubated with the PSs (0.8 μM) for 24 hours and analyzed using ImageStream^x (Ex. 405 nm, Em. 740-800 nm). **(A)** Uptake of **3** and both the isomers was measured by flow cytometry **(B)** Subcellular distribution of **3** as isomeric mixture in mitochondria (red) and lysosome (green). Distribution was measured in terms of similarity score which is a measure of co-localization with mitochondrial (CMXRos - Ex. 561 nm Em. 595-660 nm) or lysosome (Green Fluorospheres - Ex. 488 nm Em. 480-560 nm). The more positive the similarity score the more closely the fluorescent probes are co-localized. Both A and B are the average of **3** experiments done in duplicate, error bars represent standard deviation, $p<0.05$. **(C)** *In vitro* PDT activity of **3** (red), isomer **3a** (green), and isomer **3b** (blue) was determined by using the cell viability MTT assay. Colon 26 cells were incubated with 0.025 μM compound for 24 hours and then irradiated with a laser light (787 nm) at various doses of light (0 – 1.0 J/cm^2). Values are expressed as cell percent survival (set to 100%). Data represents the results of a single experiment in triplicate, error bars represent standard deviation.

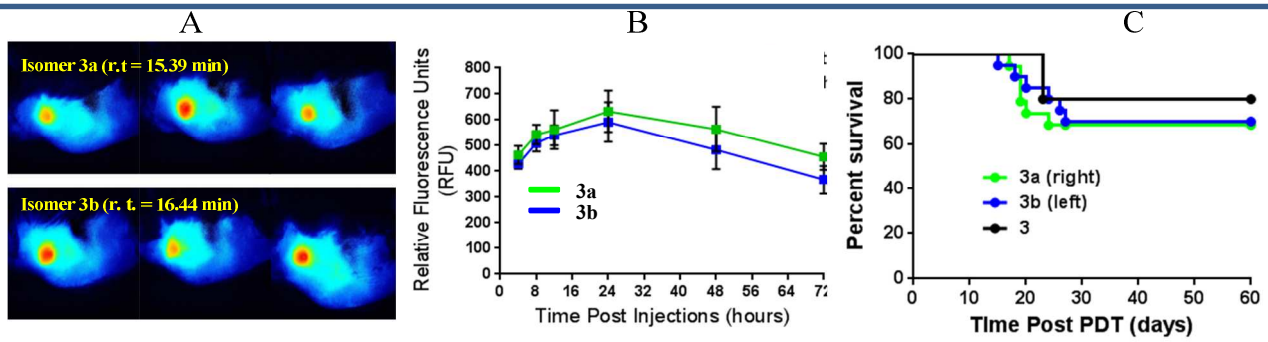

Figure 10: (A) Whole body fluorescence images of BALB/c mice bearing Colon26 tumors (3 mice/group) injected with isomer **3a** (upper row) and **3b** (lower row) at a dose of 0.25 μmol/kg (therapeutic dose) and imaged at 24h post-injection. **(B)** Comparative uptake of **3a** (green) and **3b** (blue) in Balb/c mice (3 mice/group) at variable time points. Both isomers produced maximal uptake at 24 h post-injection. **(C)** Comparative *in vivo* PDT efficacy of bacteriopurpurinimide **3** and its stereoisomers **3a** and **3b** in BALB/c mice bearing Colon 26 tumors (10 mice/group) at a dose of 0.25 mmol/kg treated with light (787 nm, 135 J/cm^2, 75 mW/cm^2) at 24 h post-injection. Tumor regrowth was monitored for day 60. PS **3** and its stereoisomers **3a** and **3b** showed similar tumor cure (8/10 mice in each group were tumor free on day 60. Retention time (r.t): **3a** = 15.39 min, **3b** = 16.94 min.

lysosomes. To correlate the cellular uptake of the isomers to PDT efficacy *in vitro*, a series of MTT assay was performed using Colon26 tumor cells incubated with the photosensitizers for 24h under similar PS concentrations and light doses. The results summarized in **Figure 9C** show the *in vitro* PDT efficacy from a single PS concentration (0.025 μM) and the cells were exposed to light at 787 nm in the range of 0-1.0 J/cm^2, and no significant difference in photosensitizing ability was observed.

For investigating *in vivo* efficacy, similar experiments with these isomers were then extended in BALB/c mice bearing Colon26 tumors and the results are depicted in **Figure 10**. As indicated, both isomers showed maximal tumor-uptake at 24 h post-injection with a similar clearence profile (**Figure 10B**). The isomeric mixture and the individual isomers were also evaluated for *in vivo* PDT efficacy. The results illustrated in **Figure 10C** showed similar long-term tumor cure by the isomeric mixture and the individual isomers.

Compared to chlorins (HPPH 1 and purpurinimide 2), bacteriopurpurinimide (3) shows enhanced PDT efficacy:

Among the chlorins with long wavelength absorption in the range of 660 to 700 nm evaluated in our laboratories, (665 nm) **1** (665 nm) and **2** (702 nm) were noted to mediate effective PDT in several tumor models.[25] To rate these PS against **3**, *in vivo* biological efficaces of HPPH **1,** purpurinimide **2** and **3** were assessed under identical conditions. The results summarized in **Figure 11** indicate that the PDTefficacy ranked as **3** > **2** > **1**.

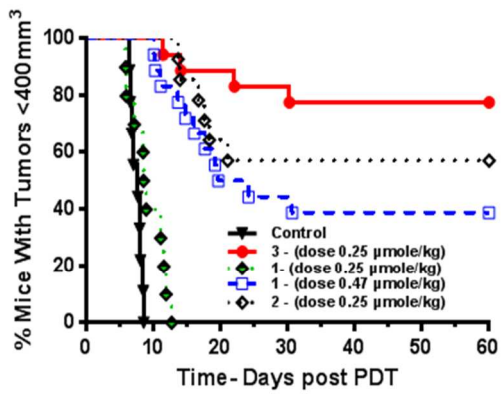

Figure 11: Comparative in vivo PDT efficacy of **1, 2** and **3** in BALB/c mice bearing Colon26 tumors. Compound 1 at a dose of 0.25 and 0.47 μmol/kg (665 nm) purpurinimide **2** (702 nm) and bacteriopurpurinimide **3** at a dose of 0.25 μmol/kg was injected in tumored mice. The tumors were exposed to light (787 nm, 135 J/cm^2, 75 mW/cm^2) at 24 h post-injection (optimal drug uptake time point for all the photosensitizers). As per approved protocol, mice with tumor >400 mm^3 should be sacrificed. However, compounds 3, 2 and 1 gave 80%, 60% and 40% complete cure Mice with no tumors) respectively.

Injecting compounnd **1** at the higher dose (0. 47 mmol/Kg), yielded 40% tumor cure. To confirm that the longer wavelength of light alone has no impact on tumor inhibition, the tumors (3 mice/group) were irradiated with light at therapeutic wavelength 665, 702 or 787 nm of PSs **1, 2** and **3** respectively, and no tumor inhibition was observed (see **Figure S21,** Supplemental Information).

Fluorescence imaging of lung tumors with PS 3: To further expand the imaging capability of **3**, we experimentally introduced tumors into the lungs of the mice (BALB/c, 3 mice/group) by injecting 4T1-luc cells intravenously. After 9 days of tumor implantation, the bioluminescence images of tumors were recorded. Compound **3** (0.25 μmole/kg) was then injected to mice intravenously and the fluorescence images of tumors were obtained after 24 h by IVIS Spectrum-CT. It also showed high tumor-avidity and made it possible to locate the tumors implanted in the lungs. The multi-modal image (fluorescence (red) merged with bioluminescence (blue) = pink) shows the localization of **3** within the tumor. The intensity of the localization matched with the epi-fluorescence of the PS, which further indicates excellent tumor specificity (**Figure 12**).

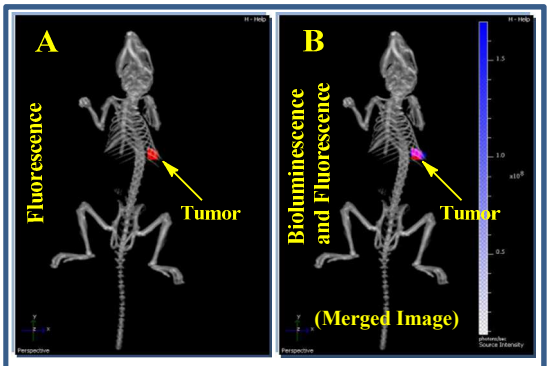

Figure 12: Bioluminescence images of tumors were taken at day-9 after injecting (*i. v.)* 4T1-luc tumor cells in BALB/c mouse**.** Mice were injected with **3** (0.25 μmol/kg) and the fluorescence images (Ex. 785 nm, Em. > 830 nm) of tumors were recorded at 24h post-injection (**A**). The merged image (pink) (fluorescence–red, + bio luminescence-blue) shows the tumor-specificity of **3** (**B**). The imaging experiment was performed at the Pekin-Elmer Imaging Facility, California, USA.

Photobleaching of compound 3 *in vivo:*

To determine the rate of photobleaching[30-32] of compound **3** during the *in vivo* light treatment, BALB/c mice bearing Colon26 tumors were injected with 0.25 mmol/kg of the photosensitizer and the fluorescence intensity of **3** from the tumor (*in situ*) was recorded prior to light-irradiation (t = 0) and used as 100% value for each mouse. The tumors were then exposed to 787 nm light and in regular interval the irradiation was stopped. The fluorescence intensity

was recorded, and the light treatment was continued. This procedure was repeated until the total time of combined light treatment reached 30 min. The percentage of fluorescence observed in the tumor was plotted against the time of exposure with light. The results obtained are summarized in **Figure 13** indicate an initial rapid rate of photobleaching of the PS, followed by a decreased rate of photobleaching with approximately 40% of the photosensitizer fluorescence still present (not photo-bleached) after the light exposure used for PDT. However in this study, in contrast to a continued light exposure during the PDT treatment, the light treatment was stopped at regular intervals for determining the photo-bleaching of the PS by fluorescence, which may help in re-oxygenating the tumor tissue. To avoid tissue re-oxygenation, the fluorescence measurement of the PS in tumors before and after the PDT treatment was performed in a separate set of animals, and a very similar end results were observed (data not shown).

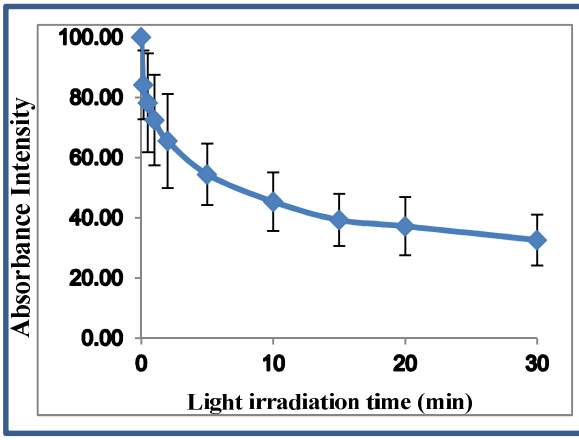

Figure 13: *In vivo* photobleaching of **3**. BALB/c mice (3) bearing colon 26 tumors were irradiated at 24 hours after injection of **3** (dose, 0.25 μmol/kg with 797 nm light (135 J/cm^2 at 75 mW/cm^2). At regular intervals of a 30 minute span, mice were imaged with Maestro Deep Red filter set for PS signal which was plotted against pre-irradiated signal (the decay of the absorption band at 787 nm at each time point was measured and plotted with time). The data presented are from a single experiment, error bars represent standard deviation, $p<0.05$.

STAT3 photo-induced dimerization correlates to PDT response:

Previous reports from our laboratory have shown that murine and human cancer cell lines react to PDT treatment by an immediate covalent cross-linking of STAT3 to homodimeric and other complexes[33]. A direct correlation between the photo-induced STAT-3 dimerization after irradiating the cells with light and concentration of the photosensitizer (PS) was observed.[34] The light dose did produce a significant difference in cross-linking of STAT3, but light alone, or

PS alone did not had any impact in cell death. To further correlate the *in vitro* and *in vivo* PDT response of **3** and the corresponding carboxylic acid **10,** Colon26 cells were incubated with either **3** or **10** were exposed to light at 787 nm and quantified the light-dependent STAT3 cross-linking by Western blot. The data summarized in **Figure 14,** clearly indicates that compound **10,** which was more effective *in vitro* than **3,** showed higher STAT 3 dimerization. However, *in vivo* PS **3**, which produced higher uptake and long-term tumor cure than **10,**

also showed a direct correlation with higher STAT3 dimerization

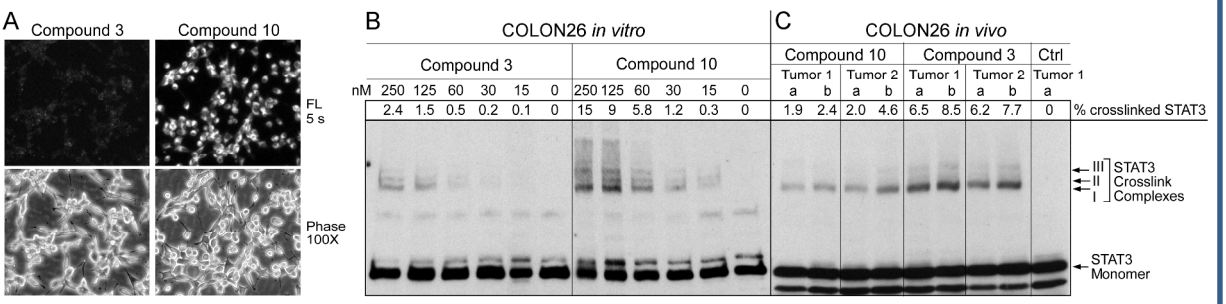

Figure 14: A, Cell-associated compounds **3** and **10** were visualized by fluorescent microscopy in Colon26 cell cultures incubated for 2 h in medium containing 3200 nM photosensitizer. Phase and fluorescent images of the cultures at 100X magnification are shown. **B** & **C,** Photoreaction mediated by compounds **3** and **10** in Colon26 cells *in vitro* and *in vivo*. Crosslinking of STAT3 as measure for photosensitizing activity. **Left panel (B)**: Colon26 cell monolayers were incubated for 24 hours in culture medium containing the indicated concentrations of compounds **3** and **10**. After washing the cultures with serum-free medium, the cells were treated with 797-nm light (3 J/cm^2) and immediately extracted. **Right panel (C)**: Mice bearing a Colon26 tumor(~6-8 mm largest dimension) were injected with compounds **3** or **10** (0.47 μmol/Kg). After 24 hours, the tumors were treated in situ with 787-nm light (---) and then immediately excised, Each tumor mass was cut into two parts (**a** and **b**) and extracted. Aliquots for the extracts from tissue cell cultures and from the tumor pieces, containing equal amount of proteins (40 μg), were analyzed by Western blotting for STAT3. The percent conversion of monomeric STAT3 into homodimeric crosslinked STAT3 was calculated and indicated at the top each lane.

Compound 3 produces limited skin phototoxicity:

To investigate the skin phototoxicity of **3,** non-tumor bearing mice were injected with the therapeutic dose (0.25 μmol/kg) of **3**. A various times of post-injection (day 1 to 7) one of the hind feet of each mice (3 mice/group/time point) was irradiated with solar light, the other foot was used as a control[35]. The severity of the skin reaction was graded according to Table 1 (Experimental Section) and a foot response score was assigned to each mouse[36]. Mice were

scored daily and the average foot response was plotted against the day of light treatment. The results summarized in **Fig. 15** indicate that mice treated with laser light at 24 h after injecting the PS had the strongest PDT response and were classified as moderate to strong edema. Re-examination 24 h later showed that the feet were healing and after an additional 48h the feet of these mice returned to pretreatment level. Mice treated with light at 48-96 h post-injection had a less severe response than the 24 h post-injection group, and in all cases the mice responded well and their feet returned to pre-treatment level by 4-5 days of post-treatment. These results are similar to those observed for **1**, which shows limited skin phototoxicity not only in Colon26 bearing mouse model, but also in patients undergoing PDT treatment.[31]

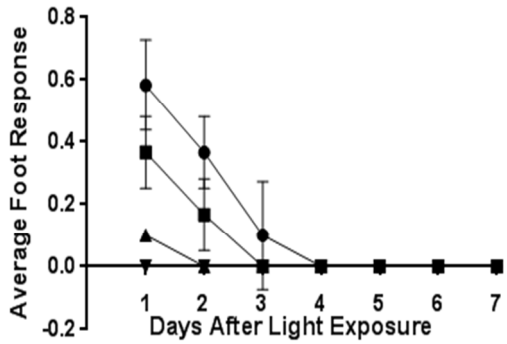

Figure 15: Skin phototoxicity assessment of NIR PS **3**. BALB/c mice were injected at a dose of 0.25 μmol/kg (therapeutic dose). At intervals of 24 h (circle), 48 h (square), 72 h (triangle) and 96 h (diamond) post injection mice were restrained and one hind foot was illuminated with solar light for 30 min. The foot response for each mouse (3 mice/ group) was observed and scored ranging from 0 (no apparent difference from normal untreated foot) to 3 (loss of foot). Data plotted are from a single experiment, error bars represent standard deviation.

1.1. Determination of logP values of 3 and 10

The Pallas program[37] which is currently well-accepted in drug development by most of the pharmaceutical companies was used to determine the logP values. The calculated logP values for photosensitizers **3** and **10** are 6. 32 and 6.11 respectively.

Stability of methyl ester functionality of 3 in biological media

To confirm the stability of ester group in PS **3** in biological media, the compound was incubated in Colon26 cells for 24 h, the media was removed and the cells were washed. Methanol was then added to cells, stirred and centrifuged. The pallet of cells was removed. The solvent was concentrated by blowing a slow stream of nitrogen. It was then chromatographed in analytical TLC with compounds **3** (methyl ester) and **10** (carboxylic acid), The hydrolysis of

methyl ester to carboxylic acid was not observed (**Figure S22**, **Supplemental Information**). The metabolic studies of PS **3** at variable doses in rats and dogs (GLP facility) following the US FDA guidelines are underway.

CONCLUSION

Our present study indicates that the presence and nature of the fused exocyclic ring structure in the tetrapyrrolic system makes a significant difference in photophysical characteristics of the compounds. For example **1,** a pyropheophorbide-a analog containing a five member isocyclic ring shows long wavelength absorption in methanol at 660 nm, whereas the purpurinimide **2** in which the five member ring is replaced with a six member imide ring system exhibits its long wavelength absorption near 700 nm. Reducing the ring 'B' of purpurinimide **2** to produce bacteriopurpurinimide **3** further extends its long wavelength absorption to 782 nm, a shift of 87 nm with a remarkable difference in the Stokes shift between the absorption and fluorescence emission. The *in vivo* data (imaging and therapy) discussed in this manuscript are based on a large number of tumor bearing mice in several groups and indicate the potential of **3** in long-term tumor cure than that achieved by **1** and **2**. The inherent more favorable optical and biological properties render compound **3** as a NIR fluorophore for image-guided surgery with an option of photodynamic treatment to a variety of tumor types, and these studies are currently underway. The fundamental comparison of carboxylic acid and methyl ester derivatives has also revealed a striking difference in pharmacokinetic properties that remain to be defined. Similar to most of the porphyrin-based compounds, as expected, **3** also showed photobleaching characteristics on irradiating with light. However, more than 50% of the PS was still available at post-treatment time, which again makes it a suitable candidate for PDT.

On the basis of ease of synthesis, *in vivo* biological efficacy and photophysical characteristics of the bacteriochlorin-based photosensitizers developed so far in our laboratory, **3** is the most promising dual-function NIR agent for fluorescence guided PDT.[38-40]

EXPERIMENTAL SECTION

1. Chemistry Methods.

1.1 Synthesis. All reactions were carried out in heat gun-dried glassware, under an atmosphere of nitrogen and magnetic stirring. Thin-layer chromatography (TLC) was done on precoated silica gel sheets (layer thickness: 0.25 mm) or aluminum oxide sheets. Column chromatography was performed either using silica gel 60 (70-230 mesh) or neutral alumina grade III. In some cases preparative TLC was used for the purification of compounds. Solvents were dried following the standard methodology. Purity of the compounds was ascertained by TLC or by HPLC analyses. All compounds (including the intermediates were >95% pure. ^{1}H NMR spectra were recorded at room temperature in $CDCl_3$ solution using either a Varian VNMRS-400 spectrometer or a Bruker Avance III 400 spectrometer. All chemicals shifts are reported in parts per million (δ). ^{1}H NMR (400 MHz) spectra were referenced to residual $CHCl_3$ (7.26 ppm) or TMS (0.00 ppm). ^{13}C NMR (100 MHz) spectra were referenced to $CDCl_3$ (77.02 ppm) or TMS (0.00 ppm). Mass spectrometry analyses were performed at the Mass Spectrometry Facility, Michigan State University, East Lansing. UV-visible spectra were recorded on FT UV-visible spectrophotometer using dichloromethane/THF as solvent.

3^{1}-(1-Butoxy)ethyl-3-deacetylbacteriopurpurin-18-N-butylimide Methyl Ester **(3):** Bacteriochlorin **8** (40 mg) was dissolved in dry dichloromethane (5.0 mL). HBr gas was bubbled through the solution for 2 min, and stirred at room temperature under an argon atmosphere for 5 min. The solvent and the excess hydrogen bromide were then evaporated under anhydrous high vacuum (at or below 30 °C) to give a residue, which was immediately redissolved in dry dichloromethane (10 mL) and *n*-butanol (0.6 mL to give 100 fold excess, Sigma Aldrich, St. Louis, MO and American Radiolabeled Chemicals, St. Louis, MO for radioactive) in the presence of anhydrous potassium carbonate (200mg). The reaction mixture was stirred for 30 min. After the standard workup, the residue was purified on PTLC using Ethyl acetate/Hexanes (40% v/v), and the title compound was obtained in as a solid. Yield 35 mg (83%). UV-vis (CH_2Cl_2, λ_{max}, nm, (ε)): 355,

366, 416, 472, 537, 702, 787 (5.44 x10^4); ^{1}H NMR (400 MHz, $CDCl_3$, δ ppm): 8.83/8.78 (s, 1H, 5-H), 8.60 (s, 1H, 10-H), 8.31 (s, 1H, 20-H), 5.66/5.64 (q, 1H, 3^1-H, *J* = 6.7 Hz), 5.25 (m, 1H, 17-H), 4.42 (m, 2H, -NC*H*$_2$(CH$_2$)$_2$CH$_3$), 4.11-4.23 (m, 2H, 1H for 7-H, 1H for 18-H), 4.00 (m, 1H, 8-H), 3.62 (s, 3H, 12-CH$_3$), 3.562/3.561 (s, 3H, -COOC*H*$_3$), 3.48-3.63 (m, 2H, OC*H*$_2$CH$_2$CH$_2$CH$_3$), 3.23/3.22 (s, 3H, 2-CH$_3$), 2.63 (m, 1H, -CH$_2$C*H*HCOOMe), 2.22-2.42 (m, 3H, 1H for -C*H*HCH$_2$COOMe, 1H for 8-C*H*HCH$_3$, 1H for -CH$_2$CH*H*COOMe), 1.99 (d, 3H, 3^1-CH$_3$, *J* = 6.6 Hz), 1.88-2.12 (m, 4H, 1H for 8-CH*H*CH$_3$, 1H for 17-CH*H*CH$_2$COOMe, 2H for -NCH$_2$C*H*$_2$CH$_2$CH$_3$), 1.79/1.78 (d, 3H, 7-CH$_3$, *J* = 7.1 Hz), 1.66-1.73 (m, 2H, OCH$_2$C*H*$_2$CH$_2$CH$_3$), 1.69 (d, 3H, 18-CH$_3$, *J* = 7.3 Hz), 1.62 (m, 2H, -NCH$_2$CH$_2$*CH*$_2$CH$_3$), 1.30-1.52 (m, 2H, OCH$_2$CH$_2$C*H*$_2$CH$_3$), 1.13/1.10 (t, 3H, 8-CH$_2$C*H*$_3$, *J* = 7.4 Hz), 1.08 (t, 3H, -N(CH$_2$)$_3$C*H*$_3$, *J* = 7.4 Hz), 0.86/0.85 (t, 3H, OCH$_2$CH$_2$CH$_2$*CH*$_3$, *J* = 7.4 Hz), 0.05 (s, 1H, NH), -0.32 (s, 1H, NH); ^{13}C NMR (100 MHz, $CDCl_3$, δ ppm): 173.97, 173.81/173.79, 172.41, 170.44/170.37, 167.73, 163.92, 160.89/160.84, 141.12/141.03, 138.26/138.20, 137.63/137.62, 133.26, 132.48/132.46, 131.51/131.50, 129.42/129.41, 113.97/113.96, 101.37/101.35, 99.78/99.77, 99.31/99.13, 94.76/94.73, 72.56/72.37, 69.42/69.26, 55.36/55.26, 53.76/53.73, 51.47, 49.33, 48.25/48.23, 40.03, 32.28/32.22, 32.22/32.17, 31.24, 31.11, 30.29/30.20, 24.47/24.33, 23.57/23.55, 22.87/22.71, 20.77, 19.57/19.55, 14.07, 13.93, 11.92, 10.85/10.82, 10.81/10.68. HRMS (ESI) for $C_{42}H_{56}N_5O_5$ [MH^+] calculated: 710.4266; found: 710.4282. Elemental analysis calculated for $C_{42}H_{55}N_5O_5$, C 71.06, H 7.81, N 9.87. Found: C 71.29, H 8.10, N 9.84.

Besides the desired major compound **3**, a minor product **9** in 5-7% yield was also isolated and was identified as 3-vinyl-bacteriopurpuin-18-N-butylimide methyl ester, possibility obtained by dehydration or dehyrobromination of the starting material or the intermediate unstable bromoderivative. ^{1}H NMR (400 MHz, $CDCl_3$, δ ppm): 8.62 (s, 1H, meso-H), 8.49 (s, 1H, meso-H), 8.38 (s, 1H, meso-H), 7.77 (dd, 1H, 3^1-H, *J* = 11.5, 17.9 Hz), 6.18 (dd, 1H, 3^2-H, *J* = 1.3, 17.9 Hz), 6.07 (dd, 1H, 3^2-H, *J* = 1.4, 11.6 Hz), 5.26 (m, 1H, 17-H), 4.43 (m, 2H, -

NC*H*$_2$(CH$_2$)$_2$CH$_3$), 4.15-4.24 (m, 2H, 1H for 7-H, 1H for 18-H), 4.02 (m, 1H, 8-H), 3.63 (s, 3H, 12-CH$_3$), 3.57 (s, 3H, -COOC*H*$_3$), 3.28 (s, 3H, 2-CH$_3$), 2.65 (m, 1H, -CH$_2$C*H*HCOOMe), 2.25-2.43 (m, 3H, 1H for -C*H*HCH$_2$COOMe, 1H for 8-C*H*HCH$_3$, 1H for -CH$_2$CH*H*COOMe), 1.88-2.11 (m, 4H, 1H for 8-CH*H*CH$_3$, 1H for 17-CH*H*CH$_2$COOMe, 2H for -NCH$_2$C*H*$_2$CH$_2$CH$_3$), 1.79 (d, 3H, 7-CH$_3$, *J* = 7.2 Hz), 1.70 (d, 3H, 18-CH$_3$, *J* = 7.3 Hz), 1.62 (m, 2H, -NCH$_2$CH$_2$C*H*$_2$CH$_3$), 1.11 (t, 3H, 8-CH$_2$C*H*$_3$, *J* = 7.4 Hz), 1.08 (t, 3H, -N(CH$_2$)$_3$C*H*$_3$, *J* = 7.4 Hz), 0.01 (s, 1H, NH), -0.34 (s, 1H, NH); ^{13}C NMR (100 MHz, CDCl$_3$, δ ppm): 174.0, 173.5, 172.5, 170.3, 167.7, 163.9, 161.0, 141.1, 138.2, 134.0, 133.4, 131.7, 131.6, 129.8, 128.7, 122.4, 114.1, 101.4, 99.7, 98.4, 95.3, 55.4, 53.8, 51.5, 49.3, 48.2, 40.0, 32.3, 31.3, 31.1, 30.2, 23.6, 22.8, 20.8, 14.1, 11.94, 11.92, 10.7. HRMS (ESI) for $C_{38}H_{46}N_5O_4$ [MH$^+$] calculated: 636.3584; found: 636.3541. HPLC retention time: 13.73 min (see Figure S20b, purity > 96.4% Supplemental Information).

1.2 HPLC Method for the separation of isomers present in bacteriopurpurinimde 3a and Isomer 3b. The purity of isolated isomers **3a** and **3b** eluted by column chromatography were injected on an analytical column (Waters C18 Symmetry, 4.6 x 150 mm, 5 m particle size), mobile phase 100% methanol at 1.0 ml/min). The retention times of **3a** and **3b** were 15.39 min and 16.44 min respectively.

Isomer **3a** *(retention time 15.39 min):* UV-vis (MeOH, λ_{max}, nm, (ε)): 344, 366, 416, 537, 702, 780 (4.73 x10^4); ^{1}H NMR (400 MHz, CDCl$_3$, δ ppm): 8.79 (s, 1H, 5-H), 8.60 (s, 1H, 10-H), 8.31 (s, 1H, 20-H), 5.66 (q, 1H, 3^1-H, *J* = 6.7 Hz), 5.25 (m, 1H, 17-H), 4.42 (m, 2H, -NC*H*$_2$(CH$_2$)$_2$CH$_3$), 4.11-4.23 (m, 2H, 1H for 7-H, 1H for 18-H), 4.01 (m, 1H, 8-H), 3.62 (s, 3H, 12-CH$_3$), 3.47-3.64 (m, 2H, OC*H*$_2$CH$_2$CH$_2$CH$_3$), 3.563 (s, 3H, -COOC*H*$_3$), 3.23 (s, 3H, 2-CH$_3$), 2.63 (m, 1H, 17-CH$_2$C*H*HCOOMe), 2.21-2.42 (m, 3H, 1H for -C*H*HCH$_2$COOMe, 1H for 8-C*H*HCH$_3$, 1H for 17-CH$_2$CH*H*COOMe), 2.00 (d, 3H, 3^1-CH$_3$, *J* = 6.6 Hz), 1.88-2.12 (m, 4H, 1H for 8-CH*H*CH$_3$, 1H for 17-CH*H*CH$_2$COOMe, 2H for -NCH$_2$C*H*$_2$CH$_2$CH$_3$), 1.79 (d, 3H, 7-CH$_3$, *J* = 7.2 Hz), 1.66-1.77 (m, 2H, OCH$_2$C*H*$_2$CH$_2$CH$_3$), 1.69 (d, 3H, 18-CH$_3$, *J* = 7.3 Hz), 1.62 (m, 2H, -NCH$_2$CH$_2$C*H*$_2$CH$_3$), 1.31-1.52 (m, 2H, OCH$_2$CH$_2$C*H*$_2$CH$_3$), 1.10 (t, 3H, 8-CH$_2$C*H*$_3$, *J* = 7.4 Hz), 1.08 (t, 3H, -

$N(CH_2)_3CH_3$, *J* = 7.4 Hz), 0.86 (t, 3H, $OCH_2CH_2CH_2CH_3$, *J* = 7.4 Hz), 0.05 (s, 1H, NH), -0.32 (s, 1H, NH); ^{13}C NMR (100 MHz, $CDCl_3$, δ ppm): 173.99, 173.81, 172.41, 170.38, 167.72, 163.92, 160.83, 141.11, 138.18, 137.60, 133.24, 132.48, 131.49, 129.41, 113.93, 101.35, 99.76, 99.13, 94.75, 72.35, 69.25, 55.24, 53.74, 51.49, 49.30, 48.24, 40.03, 32.20, 32.16, 31.21, 31.10, 30.21, 24.34, 23.55, 22.88, 20.77, 19.57, 14.08, 13.93, 11.93, 10.85, 10.68; MS (ESI): *m*/*z* 710 (M^+). HPLC chromatograms: (Figure 3 of the main text, purity > 99%).

*Isomer **3b** (retention time: 16.94 min):* UV-vis (MeOH, λ_{max}, nm, (ε)): 344, 366, 416, 537, 702, 780 (4.73 x10^4); ^{1}H NMR (400 MHz, $CDCl_3$, δ ppm): 8.83 (s, 1H, 5-H), 8.59 (s, 1H, 10-H), 8.31 (s, 1H, 20-H), 5.64 (q, 1H, 3^1-H, J=6.7 Hz), 5.25 (dd, 1H, 17-H, J=2.8, 8.8 Hz), 4.42 (m, 2H, -$NCH_2(CH_2)_2CH_3$), 4.14-4.23 (m, 2H, 1H for 7-H, 1H for 18-H), 4.00 (m, 1H, 8-H), 3.62 (s, 3H, 12-CH_3), 3.59 (m, 1H, $OCHCH_2CH_2CH_3$), 3.560 (s, 3H, -$COOCH_3$), 3.52 (m, 1H, $OCHCH_2CH_2CH_3$), 3.22 (s, 3H, 2-CH_3), 2.63 (m, 1H, -CH_2CHHCOOMe), 2.21-2.42 (m, 3H, 1H for -CHHCH$_2$COOMe, 1H for 8-CHHCH$_3$, 1H for -CH_2CHHCOOMe), 1.99 (d, 3H, 3^1-CH_3, J=6.7 Hz), 1.87-2.12 (m, 4H, 1H for 8-CHHCH_3, 1H for 17-CHHCH_2COOMe, 2H for -$NCH_2CH_2CH_2CH_3$), 1.77 (d, 3H, 7-CH_3, *J* = 7.2 Hz), 1.65-1.73 (m, 2H, $OCH_2CH_2CH_2CH_3$), 1.69 (d, 3H, 18-CH_3, *J* = 7.3 Hz), 1.61 (m, 2H, -$NCH_2CH_2CH_2CH_3$), 1.38 (m, 2H, $OCH_2CH_2CH_2CH_3$), 1.12 (t, 3H, 8-CH_2CH_3, *J* = 7.4 Hz), 1.08 (t, 3H, -$N(CH_2)_3CH_3$, *J* = 7.4 Hz), 0.85 (t, 3H, $OCH_2CH_2CH_2CH_3$, *J* = 7.4 Hz), 0.05 (s, 1H, NH), -0.32 (s, 1H, NH); ^{13}C NMR (100 MHz, $CDCl_3$, δ ppm): 173.99, 173.79, 172.41, 170.45, 167.72, 163.92, 160.88, 141.02, 138.24, 137.62, 133.25, 132.49, 131.48, 129.40, 113.93, 101.37, 99.74, 99.32, 94.73, 72.55, 69.42, 55.34, 53.71, 51.48, 49.31, 48.21, 40.03, 32.27, 32.20, 31.21, 31.11, 30.29, 24.48, 23.57, 22.72, 20.77, 19.55, 14.08, 13.94, 11.93, 10.82, 10.81; MS (ESI): *m*/*z* 710 (M^+). HPLC Chromatograms: (Figure 3 of the main text, purity > 99%).

*3-Acetylbacteriopurpurin-18-N-butylimide Methyl Ester **(7):*** 3-Acetylbacteriopurpurin-18 methyl ester **6** was prepared from methyl bacteriopheophorbide-*a* **4** following a published procedure.[27] 3-Acetylbacteriopurpurin-18 methyl ester **6** (300 mg) dissolved in CH_2Cl_2 (25 mL) was treated

with a butylamine (4.0 mL) at room temperature for 18 h. The disappearance of the absorption at 813 nm and the appearance of a new absorption peak at 753 nm indicated the formation of the intermediate amide system. The reaction mixture was then treated with diazomethane for 10 min and then diazomethane was removed by passing argon through it for 30 min. This was further treated with a catalytic amount of methanolic KOH was added and the mixture was stirred for 1-2 min. The disappearance of the absorption at 753 nm and appearance of a new peak 822 nm indicated the completion of the reaction. Following the standard workup, the residue was chromatographed over a grade III alumina column eluting with 30% hexanes/CH_2Cl_2. The appropriate fractions were combined. Yield 176 mg (53%). UV-vis (CH_2Cl_2, λ_{max}, nm): 363, 414, 546, 753, 822; ^{1}H NMR (400 MHz, $CDCl_3$, δ ppm): 9.23 (s, 1H, 5-H), 8.81 (s, 1H, 10-H), 8.63 (s, 1H, 20-H), 5.31 (m, 1H, 17-H), 4.44 (m, 2H, -NC*H*$_2$(CH$_2$)$_2$CH$_3$), 4.23-4.34 (m, 2H, 1H for 7-H, 1H for 18-H), 4.11 (m, 1H, 8-H), 3.70 (s, 3H, 12-CH_3), 3.57 (s, 3H, -COOC*H*$_3$), 3.55 (s, 3H, 2-CH_3), 3.17 (s, 3H, $COCH_3$), 2.68 (m, 1H, -CH_2C*H*HCOOMe), 2.28-2.43 (m, 3H, 1H for -C*H*HCH_2COOMe, 1H for 8-C*H*HCH_3, 1H for -CH_2CH*H*COOMe), 2.07 (m, 1H, 8-CH*H*CH_3), 1.89-2.02 (m, 3H, 1H for 17-CH*H*CH_2COOMe, 2H for -NCH_2C*H*$_2$$CH_2$$CH_3$), 1.82 (d, 3H, 7-$CH_3$, *J*=7.3 Hz), 1.73 (d, 3H, 18-CH_3, *J*=7.3 Hz), 1.63 (m, 2H, -N$CH_2$$CH_2$*CH*$_2$$CH_3$), 1.11 (t, 3H, 8-$CH_2$C*H*$_3$, *J*=7.4 Hz), 1.09 (t, 3H, -N(CH$_2$)$_3$C*H*$_3$, *J*=7.4 Hz), -0.52 (s, 1H, NH), -0.73 (s, 1H, NH); ^{13}C NMR (100 MHz, $CDCl_3$, δ ppm): 198.6, 173.9, 172.8, 169.74, 169.73, 167.5, 164.5, 163.5, 136.5, 135.6, 135.4, 134.7, 134.3, 133.7, 131.7, 116.3, 101.9, 101.7, 99.2, 97.1, 56.4, 54.4, 51.5, 48.5, 47.5, 40.1, 33.2, 32.3, 31.2, 31.1, 30.0, 24.0, 23.3, 20.7, 14.1, 13.6, 12.2, 10.8. HRMS (ESI) for $C_{38}H_{46}N_5O_5$ [MH^+] calculated: 652.3457; found: 652.3492. Elemental analysis calculated for $C_{38}H_{45}N_5O_5$, C 70.02, H 6.96, N 10.74. Found: C 69.88, H 6.86, N 10.57.

3-(1-Hydroxy)ethyl-3-deacetylbacteriopurpurin-18-N-butylimide Methyl Ester ***(8):*** Bacteriochlorin **7** (170 mg) was dissolved in 25 mL CH_2Cl_2. Sodium borohydride (360mg) in two lots was added and 3 mL methanol were added to the reaction mixture. The reaction was monitored by TLC and UV-vis spectrophotometry. The disappearance of the 822 nm band and the appearance of

a new band at 787 nm indicated the completion of the reaction (reaction time: 20 min). This was then neutaralized using 2% acetic acid/water and then extracted with CH2Cl2.(3X100ml), dried over sodium sulphate and concentrated at rotary evaporator to give **8**. Yield quantitative. UV-vis (CH_2Cl_2, λ_{max}, nm): 366, 417, 534, 726, 787; ^{1}H NMR (400 MHz, $CDCl_3$, δ ppm): 8.82/8.80 (s, 1H, 5-H), 8.61 (s, 1H, 10-H), 8.33 (s, 1H, 20-H), 6.21 (q, 1H, 3^1-H, J=6.6 Hz), 5.24 (m, 1H, 17-H), 4.42 (m, 2H, -NC*H*$_2$(CH_2)$_2$$CH_3$), 4.14-4.24 (m, 2H, 1H for 7-H, 1H for 18-H), 4.01 (m, 1H, 8-H), 3.62 (s, 3H, 12-CH_3), 3.57/3.56 (s, 3H, -COOC*H*$_3$), 3.27 (s, 3H, 2-CH_3), 2.63 (m, 1H, -CH_2C*H*HCOOMe), 2.52/2.50 (d, 1H, 3^1-O*H*, *J* =1.6 Hz), 2.24-2.42 (m, 3H, 1H for -C*H*HCH_2COOMe, 1H for 8-C*H*HCH_3, 1H for -CH_2CH*H*COOMe), 2.05 (d, 3H, 3^1-CH_3, *J* = 6.6 Hz), 1.88-2.10 (m, 4H, 1H for 8-CH*H*CH_3, 1H for 17-CH*H*CH_2COOMe, 2H for -NCH_2C*H*$_2$$CH_2$$CH_3$), 1.79/1.78 (d, 3H, 7-$CH_3$, *J* = 7.2 Hz), 1.69/1.68 (d, 3H, 18-CH_3, *J* = 7.3 Hz), 1.62 (m, 2H, -N$CH_2$$CH_2$*CH*$_2$$CH_3$), 1.11 (t, 3H, 8-$CH_2$C*H*$_3$, *J* = 7.3 Hz), 1.08 (t, 3H, -N(CH_2)$_3$C*H*$_3$, *J* = 7.4 Hz), -0.03 (s, 1H, NH), -0.39 (s, 1H, NH); ^{13}C NMR (100 MHz, $CDCl_3$, δ ppm): 173.99/173.97, 173.61/173.60, 172.45/172.43, 170.2, 167.7, 163.9, 161.06/161.05, 140.83/140.82, 139.17/139.14, 137.20/137.11, 133.4, 131.6, 131.49/131.45, 129.74/129.73, 114.1, 101.4, 99.75/99.74, 99.32/99.29, 94.98/94.94, 65.54/65.50, 55.4, 53.81/53.76, 51.5, 49.3, 48.22/48.18, 40.0, 32.27/32.24, 31.3, 31.1, 30.2, 25.64/25.62, 23.60/23.57, 22.90/22.82, 20.8, 14.1, 11.9, 11.13/11.11, 10.77/10.76. HRMS (ESI) for $C_{38}H_{48}N_5O_5$ [MH^+] calculated: 654.3627; found: 654.3649.

*3^1-(1-Butoxy)ethyl-3-deacetylbacteriopurpurin-18-N-butylimide carboxylic acid **(10)**:* In a dry RB flask, 60 mg of **3** was dissolved in 40 ml of dry acetonitrile and stirred well. A 650 mg of LiOH dissolved in 13 ml of water was added slowly. The entire reaction mixture was stirred overnight at room temperature. TLC after 18 hours showed some starting material. Added 100 mg of LiOH in 2ml of water and stirred for another 4 hours. The mixture was washing with 2% Acetic acid/water solvent mixture. The combined organic layer was dried over sodium sulphate and the filtrate was evaporated under reduced pressure. The crude obtained was purified by silica gel

PTLC using 55% hexanes/Ethyl acetate. Yield 24 mg (40%). UV-vis (CH_2Cl_2, λ_{max}, nm, (ε)): 365, 413, 472, 537, 701, 784 (5.44 x10^4); ^{1}H NMR (400 MHz, $CDCl_3$, δ ppm): 8.83/8.78 (s, 1H, 5-H), 8.58 (s, 1H, 10-H), 8.30 (s, 1H, 20-H), 5.64/5.62 (q, 1H, 3^1-H, *J* = 6.7 Hz), 5.22 (m, 1H, 17-H), 4.40 (m, 2H, -NC*H*$_2$(CH_2)$_2$$CH_3$), 4.10-4.23 (m, 2H, 1H for 7-H, 1H for 18-H), 3.99 (m, 1H, 8-H), 3.60 (s, 3H, 12-CH_3), 3.46-3.63 (m, 2H, OC*H*$_2$$CH_2$$CH_2$$CH_3$), 3.21/3.20 (s, 3H, 2-$CH_3$), 2.63-2.74 (m, 1H, -$CH_2$C*H*HCOOH), 2.25-2.41 (m, 3H, 1H for -C*H*HCH_2COOH, 1H for 8-C*H*HCH_3, 1H for -CH_2CH*H*COOH), 1.99/1.98 (d, 3H, 3^1-CH_3, *J* = 6.7 Hz), 1.86-2.09 (m, 4H, 1H for 8-CH*H*CH_3, 1H for 17-CH*H*CH_2COOH, 2H for -NCH_2C*H*$_2$$CH_2$$CH_3$), 1.78/1.77 (d, 3H, 7-$CH_3$, *J* = 7.1 Hz), 1.64-1.71 (m, 2H, OCH_2C*H*$_2$$CH_2$$CH_3$), 1.67 (d, 3H, 18-$CH_3$, *J* = 7.3 Hz), 1.59 (m, 2H, -N$CH_2$$CH_2$C*H*$_2$$CH_3$), 1.30-1.50 (m, 2H, O$CH_2$$CH_2$C*H*$_2$$CH_3$), 1.11/1.08 (t, 3H, 8-$CH_2$C*H*$_3$, *J* = 7.4 Hz), 1.05 (t, 3H, -N(CH_2)$_3$C*H*$_3$, *J* = 7.4 Hz), 0.85 (t, 3H, O$CH_2$$CH_2$$CH_2$C*H*$_3$, *J* = 7.4 Hz), 0.05 (s, 1H, NH), -0.31 (s, 1H, NH); ^{13}C NMR (100 MHz, $CDCl_3$, δ ppm): 177.44, 173.71/173.70, 172.21, 170.50/170.43, 167.86, 163.86, 160.92/160.87, 141.19/141.10, 138.32/138.26, 137.65/137.64, 133.22, 132.53/132.51, 131.51/131.50, 129.44/129.43, 113.91/113.90, 101.42/101.40, 99.67/99.66, 99.42/99.23, 94.76/94.74, 72.55/72.35, 69.42/69.25, 55.33/55.23, 53.76/53.74, 49.27, 48.24/48.22, 40.04, 32.26/32.15, 31.90, 31.08, 30.83, 30.26/30.18, 24.45/24.31, 23.55/23.53, 22.85/22.69, 20.72, 19.54, 14.03, 13.92/13.91, 11.90, 10.82/10.80, 10.78/10.66.; MS (ESI): *m*/*z* 695.5 (M^+). HPLC chromatograms: Retention times 9.49 and 10.00 minutes, purity: 96.52%, Figure S21c, Supplemental Information.

1.3 Formulation of the photosensitizers. **1% Tween 80**. The amount of compound and volume of solution were calculated for a desired concentration. The final solution was made to be a 1% Tween 80/D5W solution. The compound and necessary volume of Tween80 were added to a mortar and mulled to a paste. The resulting paste was allowed to sit overnight and the next day the calculated amount of D5W was added to the paste and mixed. The solution was the filtered through a 0.2 μm syringe filter and the concentration was measured spectrophotometrically. The resulting drug solutions were

stored at 4°C in the dark when not in use.

2. Cell Culture and Treatments.

2.1 Cell Maintenance. Murine Colon26 carcinoma cells were cultured and maintained in sterile RPMI-1640, containing 1xL-glutamine, supplemented with 10 % Fetal Calf Serum (FCS) (Atlanta Biologicals, triple 0.1µm filtered, Lawrenceville, GA), and 1 % Penicillin/Steptomycin/L-glutamine (P/S/l-G 10,000 I.U/ml penicillin, 10,000 µg/ml streptomycin, 29.2 mg/ml L-glutamine) maintained in a humidified incubator at 37°C in atmosphere of 5 % CO_2.

2.2 *In Vitro* Accumulation and Localization. Colon26 cells were seeded in six well plates at 1.0 × 10^5 cells per well in 2 mL complete medium. After overnight incubation at 37 °C, photosensitizers were added at 0.4 – 1.6 µM for 24 h in the dark at 37 °C with Green Fluorospheres (1/10000 dilution of stock, for lysosome staining). Prior to harvesting, cells were incubated with Chloromethyl-X-rosamine (CMXRos, for mitochondrial staining) 5 nM for 10 minutes at 37°C. The Cells were harvested and re-suspended in 60 µL of PBS containing 2% FBS. Each sample was transferred to 1.5 mL siliconized microfuge tubes, kept on ice, and 10,000 cell events were processed using the AMNIS® (Seattle, WA) Image Stream Cytometry. For comparison, single color controls were made for Fluorospheres, CMXRos, and each photosensitizer. To image the PS: Ex. 405 nm, Em. 740-800 nm; Green Fluorospheres: Ex. 488 nm Em. 480-560 nm; CMXRos: Ex. 561 nm Em. 595-660 nm). For analysis of data the IDEAS® software was used for determination of co-localization.[41]

2.3. *In Vitro* Photodynamic Therapy. Colon26 cells are plated into 96 well plates (3600 cells per well), allowed to adhere to the plate and are treated with a range of compound concentrations for 24 hours. After the 24 hour drug incubation, the cells were irradiated with light from various light sources based on wavelength of irradiation. The light source was a tunable dye laser (375; Spectra-Physics, Mt. View, CA) pumped by an argon-ion laser (171; Spectra-Physics). The dye laser was tuned to the 787 nm for treatment. Total light doses range from 0 - 1 J/cm^2 at a fluence rate of 3.2 mW/cm^2. After 48 hours post PDT treatment, MTT (3-(4,5-

dimethythiazol-2-yl)-2,5-diphenyl tetrazolium bromide) was added. The solubilized formazan product was measured spectrophotometrically using a BIOTEK EL-800 plate reader. The resulting data was processed using GEN5 software. A medium blank value was subtracted from all samples and optical density (O.D.) values of treated cells are divided by mean O.D. values of untreated cells for each light dose. Results are expressed as the percent cell survival ± SD and are plotted as percent control vs. concentration of compound or percent control vs. light dose (at one concentration) using Graph Pad Prism 5.

2.4 Photosensitizer uptake, photoreaction and STAT3 analysis. Colon26 cells were incubated in DMEM containing 10% FBS and defined concentrations of PSs for 1 or 24h at 37°C. Cell-associated PS was visualized at 100X magnification on an inverted fluorescence microscope (Zeiss Axiovert 200; excitation with 787 nm laser light and recording fluorescence at λem >800 nm. Images were captured with a Q-Imaging camera in a 16 bit/channel format using 5 sec exposure time. The photoreaction was performed by illuminating PS-treated cell cultures within a tissue culture incubator at 37°C at 797 nm light of an argon-pumped dye laser for 9 min at a dose of 5.6 mW/cm^2 to a total fluence of 3 J/cm^2. Cells were extracted immediately after light treatment. Cells or tumor tissue pieces were lysed in radioimmunoprecipitation assay (RIPA) buffer. Aliquots of extracts were subjected to Western blotting as described[32]. Briefly, samples containing 40 µg of protein were separated on 6% SDS-polyacrylamide gels and transferred to Optitran BA-S 85 reinforced nitrocellulose (Whatman GmbH, Dassel, Germany). Membranes were reacted with antibodies against STAT3 (Santa Cruz Biotechnology, Santa Cruz, CA). The immune complexes were visualized with peroxidase-coupled secondary antibodies and enhanced chemiluminescence detection (Pierce Chemicals, Rockford IL). STAT3 crosslinking was expressed by the percent conversion of monomeric STAT3 into the dimer form I of the STAT3 crosslinked complexes.[31,32]

3. Animal Treatment Strategies and Husbandry.

3.1 Animal Husbandry. All animals used in experiments were housed and cared for under the

strict guidelines of the Institutional Animal Care and Use Committee (IACUC) in the Department of Laboratory and Animal Resources (DLAR) core facility at Roswell Park Cancer Institute.

3.2 Animal and tumor systems. BALB/cAnNCr mice were obtained from Fredrick National Laboratory (Fredrick, MD). Eight- to twelve-week-old animals were inoculated subcutaneously with $1x10^6$ Colon 26 cells on the right shoulder where the fur was removed.

3.3 Fluorescence Imaging. Maestro GNIR FLEX: Spectral imaging was carried out using the Maestro GNIR FLEX (Cri Inc. Woburn, MA) spectral imaging system. Three BALB/c mice with tumor volumes of ~50 mm^3 were injected i.v. with a compound such that the final concentration of each dye was equal to 0.25 μmol compound per kg body weight of the mice. Mice were anesthetized by inhalation of isoflurane (2% in 100% oxygen) and fluorescence spectral cubes were acquired by the Deep Red pre-set filter combination (illumination light from 730 nm to 950 nm in 10 nm steps at 2 second exposure for each step, Ex. 671 nm to 705 nm, Em. 750 nm long-pass).

Unmixed images, in which background signal was subtracted, were quantified using built in Maestro software. ROIs were manually created over various sites over mice and average signal was analyzed. Whole body images were created using ImageJ software ImageJ 1.44p (NIH) software. Composite images were generated by using "Merge Channel" setting. Unmixed composite image of drug signal was set to color red while white light image of mouse was set to green.

3.4 *In Vivo* Photodynamic Therapy. PDT was performed by following the standard methodology. Briefly, when tumors reach measurable volume of ~62.5 mm^3, mice were injected (t=0) intravenously with the described PS such that final concentration of each dye would be 0.25 μmol per kg body weight of the mice. At peak drug accumulation time in the tumored mice were restrained in plexiglass holders which were designed to expose one side of the mice to open air. Tumors were irradiated with laser light at 787 nm at a fluence of 135 J/cm^2 and fluence rate of 75 mW/cm^2 for 30 minutes and then removed from laser source and return to

normal housing. The mice were monitored daily for signs of toxicity/duress and if noted, were sacrificed. The endpoint for mice implanted with tumors was regrowth after treatment to tumor volume of 400 mm^3 or 60 days post PDT without regrowth. At the time of endpoint, mice were euthanized in accordance to animal protocols.

3.5 *In Vivo* Photobleaching. When tumors reach a measurable volume of ~62.5 mm^3, the mice were injected (t=0) intravenously with the described PS in a dose response manner such that final concentration of each dye would be 0.25 μmol compound per kg body weight of the mice. After 24 hours, the mice were restrained in plexiglass holders which were designed to expose one side of mice to open air. Mice were imaged using Maestro imaging system for t=0 with 2 second exposure using Deep Red pre-set filter combination. Tumors were irradiated with a laser light at 787 nm at a fluence of 135 J/cm^2 and fluence rate of 75 mW/cm^2 for 30 minutes. At regular intervals over the 30 minute treatment time frame, the mice were removed from the laser and re-imaged with Maestro imaging system. After treatment, the mice were euthanized in accordance to animal protocols. Unmixed images, in which background fluorescence was subtracted, were quantified using built in Maestro software. ROIs were manually created over various sites of the mice and average fluorescence was analyzed.

3.6 *In Vivo* Foot Response Scale to Determine Skin Phototoxicity. The photosensitizer was injected in 12 BALB/c mice at a dose of 0.25 μmol/kg on “day 0”. One rear foot of each of the 3 mice was treated 24 hours later (on “day 1”), another 3 mice were treated 48 hours after injection (“day 2”), another group of 3 at 72 h (“day 3”), and another group of 3 at 96 h (“day 4”) with 787 nm laser light at a fluence of 135 J/cm^2 and fluence rate of 75 mW/cm^2 for 30 minutes. This allows for determination of “decay” of normal tissue photosensitivity with time after injection, a critical pharmacokinetic/pharmacodynamic property of each photosensitizer. Each mouse was then followed for an additional 96 hours (4 days) after light treatment. The mice were inspected for degree of edema (swelling), erythema (redness), epilation (hair loss), and

desquamation (flaking or sloughing of skin) and the esponses were scaled based on the following table:

Foot Score	Foot Response
0 – 0.1	No apparent difference from normal untreated foot
0.3	Slight edema
0.5	Moderate edema
0.75	Significant edema
1.0	Significant erythema with exudate
1.2	Moderate edema with slightly crusty appearance
1.5	Definite erythema
1.65	Slightly damaged and/or slught fusion of toes
2.0	Most toes are fused but no cahnge in gerenal shape of foot
2.5	Foot shapeless with no toes
3.0	Only stub of foot remaining

3.7 *In vivo* biodistribution of ^{14}C-bacteriopurpurinimide (^{14}C-3). The amount of ^{14}C-labeled photosensitizer in various tissues and organs was determined by i.v. injection of 1 μmole/kg (specific activity 4.5-5.0 μCi/μmole) of radiolabeled compound into tumor bearing mice. Fifteen mice (BALB/c mice with colon 26 tumors of ~50 mm^3) were grouped with three mice per time point plus one set of 3 mice for a control carbon count. At specified time points, mice are euthanized and the serum and 10 different organs (heart, lungs, serum, tumor, skin, liver, stomach, small intestine, spleen, and muscle) werew extracted, perfused with PBS, collected in vials, and weighed. The resulting samples were solubilized using 1 mL Solvable and incubated at 50^{o}C overnight. The samples were then cooled to room temperature and bleached with 100 uL hydrogen peroxide. After the samples were sufficiently bleached, 15 mL of Ultima Gold scintillation cocktail was added to each vial and the samples were counted in a Beckman SL6000 LL scintillation counter. The resulting data were processed using an Excel spreadsheet. Results are expressed as the sample count per minute - cpm (minus background) divided by the weight of the tissue. The results were plotted as the mean cpm/mg tissue vs each organ or tissue. The tumor-uptake data are shown in Figure 7C.

4. Photophysical Characterization:

4.1 UV-Visible Spectroscopy. UV-VIS absorption spectra of compounds were obtained using a Shimadzu UV-3600 spectrophotometer by diluting drug solutions in methanol to a final concentration of 5 μM.

4.2 Fluorescence Spectroscopy. Fluorescence spectra were obtained by using a Fluorolog-3 spectrofluorometer (782 nm excitation, 785 nm and longer emission, 1 nm slits).

4.3 Singlet Oxygen Measurements. Singlet oxygen generation was detected by its phosphorescence emission at 1270 nm. A SPEX 270M Spectrometer equipped with Hamamatsu IR-PMT was used to record the singlet oxygen phosphorescence spectra. Samples were placed in a quartz cuvette and positioned directly in front of the entrance slit of the spectrophotometer and the emission signal was collected at 90^{o} relative to the excitation laser beam. Additional long-pass filters (950 LP and 538 AELP both from Omega Optical) were used to attenuate the scattered light and fluorescence from the samples. Singlet oxygen phosphorescence decay at 1270 nm was acquired using Infinium oscilloscope (Hewlett-Packard) coupled to the output of the PMT.

4.4 Statistical Analysis. All data were analyzed using Graph Pad Prism 5 software (GraphPad Software, San Diego, CA). To test for differences between the photosensitizers, a two-tailed Student's t-test was used with Confidence Intervals of 95%. For *in vivo* photo-bleaching, triplicate data were entered using GraphPad Prism 5. Analysis was performed using the grouped analysis method.

ASSOCIATED CONTENT

Supporting Information

Copies of the NMR spectra (^{1}H & ^{13}C-) of new compounds, HPLC chromatograms of **3, 9, 10**, and a figure showing no impact on exposing the tumors at variable wavelengths of light alone (665, 702 or 787 nm) are included. This material is available free of charge via the internet at http://pubs.acs.org.

AUTHOR INFORMATION

Corresponding Author

Ravindra K. Pandey, Ph.D.

Phone: 716-845-3203

E-mail: Ravindra.pandey@roswellpark.org

ACKNOWLEDGMENTS

The financial support from the NIH (STTR grant R42 CA173980-01A1) and Photolitec, LLC, is appreciated. Nayan Patel is thankful to the Department of Molecular Pharmacology and Cancer Therapeutics for providing fellowship from the NIH funded graduate student research training grant. A partial funding from the program project grant PO1CA55791 and the RPCI's Cancer Center Support Grant from the NCI (P30CA016056) is also appreciated. We would also like to thank the Michigan State University, East Lansing, Michigan and the University at Buffalo, Amherst, NY, 14221 for the NMR and mass spectrometry analyses. The authors are highly thankful to Dr. Kevin Francis and his team at Perkin Elmer Imaging Facility, California, USA for the bioluminescence and fluorescence images of **3** illustrated in Figure 11 of this manuscript. We also appreciate the help rendered by Joseph Cacaccio, Graduate Student, RPCI in determining the stability of **3** in biological media and Dr. David Bellnier, PDT center for determining the logP values of compounds 3 and 10. The elemental analyses of new compounds were performed at Midwest Microlabs, USA.

ABBREVIATIONS USED

PS, Photosensitizer; PDT, photodynamic therapy; HPD, hematoporphyrin derivative; SAR, structure-activity relationship; QSAR, quantitative structure activity relationship; Photochlor or HPPH, 3-(1'-hexyloxy)ethyl-3-devinyl-pyropheophorbide-a; STAT, signal transducer and activator or transcription, TLC, thin layer chromatography; HPLC, high performance liquid chromatography; NIR, near infrared.

REFERENCES

1. Pandey, R. K.; Kessel, D.; Dougherty, T. J. (Eds.) *Handbook of photodynamic therapy, updates on recent applications of porphyrin-based compounds*; World Scientific: Hackensack, NJ, 2016, Chapters 1-19, pp. 3-548.
2. Henderson, B. W.; and Gollnick, S. O. Mechanistic principles of photodynamic therapy, Biomedical Photonics Handbook Volume III. Therapeutics and advanced biophotonics. In *Biomedical photonics handbook*, 2nd ed.; Vo-Dinh, Ed.; CRC Press: Boca Raton; **2015**. Chapter 1, pp. 3-30.
3. Advances in photodynamic therapy; Hamblin, M. R. and Mroz, P., Eds.; Artech House: Boston, **2008,** Chapters 1-29, pp. 1-537.
4. Zheng, G.; Pandey, R. K. Porphyrins as photosensitizers in photodynamic therapy. In *The Porphyrin Handbook*; Kadish, K. M.; Smith, K. M. and Guilard, R. Eds.; Academic Press: San Diego, **2000**; pp 157 – 230.
5. Pandey, R. K.; Goswami, L. N.; Chen, Y.; Gryshuk, A.; Missert, J. R.; Oseroff, A.; Dougherty, T. J. Nature: a rich source for developing multifunctional agents. Tumor-imaging and photodynamic therapy. *Lasers Surg. Med.* **2006,** *38*, 445-467.
6. Principles of Fluorescence Spectroscopy, 3rd ed.; Lakowicz, J. R., Ed.; Springer: New York, **2006**, Chapter 19, pp 623-673.
7. Translational multimodality optical imaging; Azar, F. S. and Intes, X., Eds.; Artech House: Boston, **2008**.Chapters 1-18, pp1-367.
8. Stolik, S.; Delgado, J. A.; Perez, A.; Anasagasti, L. Measurement of the penetration depths of red and near infrared light in human “ex vivo” tissues. *J. Photochem and Photobiol. B.* **2000**, 57, 90-93.
9. DeRosa, M. C.; Crutchley, R. J. Photosensitized singlet oxygen and its applications. *Coord. Chem. Rev*. 2002, 233, 351-371.

10. Azzouri, A-R.; Lebdai. S.; Benzaghou, F.; Steil, C. Vascular-targeted photodynamic therapy with TOOKAD Soluble in localized prostate cancer: standardization of the procedure. *World J. Urol.* **2015**, *33,* 937-944.
11. Huang, Y-Y; Hamblin, M. Stable synthetic bacteriochlorins: potent light activated anti-cancer drugs. *Curr. Org. Chem.* **2015**, *19*, 948-957.
12. Pandey, S. K.; Gryshuk, A. L.; Sajjad, M.; Zheng, X.; Chen, Y.; Abouzeid, M. M.; Charamisinau, I.; Nabi, H. A.; Oseroff, A.; Pandey, R. K. Multimodality agents for tumor imaging (PET, fluorescence) and photodynamic therapy. A possible "see and treat" approach. *J. Med. Chem.* **2005**, *48*, 6286-6295.
13. Srivatsan, A.; Wang, Y.; Joshi, P.; Sajjad, M.; Chen, Y.; Liu, C.; Thankppan, K.; Missert, J. R.; Tracy, E.; Morgan, J.; Rigual, N.; Baumann, H.; Pandey, R. K. *In vitro* cellular uptake and dimerization of Signal Transducer and Activator of Transcription-3 (STAT3) identify the photosensitizing and imaging potential of isomeric photosensitizers derived from chlorophyll-a and bacteriochlorophyll-a. *J. Med. Chem*. **2011,** *54*, 6859-6873.
14. Gupta, A.; Wang, S.; Marko, A.; Joshi, P.; Ethirajan, M.; Chen, Y.; Yao, R.; Sajjad, M.; Kopelman, R.; Pandey, R. K. Polyacrylamide-based biocompatible nanoplatform enhances the tumor uptake, PET/fluorescence imaging and anticancer activity of a chlorophyll analog. *Theranostics.* **2014**, *4,* 614-628.
15. Ma, B.; Li, G.; Kanter, P.; Lamonica, D.; Grossman, Z.; Pandey, R. K. Bifunctional HPPH-N_2S_2-^{99m}Tc conjugates as tumor-imaging agents: synthesis and biodistribution studies. *J. Porphyrins and Phthalocyanines.* **2003**, *7*, 500-510.
16. Li, G.; Slansky, A.; Dobhal, M. P.; Goswami, L. N.; Graham, A.; Chen, Y.; Kanter, P.; Alberico, R. A.; Spernyak, J.; Morgan, J.; Mazurchuk, R.; Oseroff, A.; Grossman, Z; Pandey, R. K. Chlorophyll-a analogs conjugated with aminobenzyl-DTPA as potential bifunctional agents for magnetic resonance imaging and photodynamic therapy. *Bioconjugate. Chem*. **2005**, *16*, 32-42.

17. Spernyak, J. R.; White, W. H.; Goswami, L. N.; Ethirajan, M.; Chen, Y.; Missert, J. R.; Morgan, J.; Mazurchuk R.; Pandey, R. K. Hexylether derivative of pyropheophorbide-a (HPPH) on conjugating with 3 gadolinium(III) ADTPA shows potential for in vivo tumor imaging (MR-fluorescence) and photodynamic therapy. *Bioconjugate Chem.* **2010**, 21, 828-835.
18. Nguyen, Q. T.; Tsien, R. Y. Fluorescence-guided surgery with live molecular navigation - a new cutting edge*. Nat. Rev. Cancer.* **2013***, 13,* 653-662.
19. Pandey, R. K.; Sumlin, A. B.; Potter, W. R.; Bellnier, D. A.; Henderson, B. W.; Constantine, S.; Aoudia, M.; Rodgers, M. A. J.; Smith, K. M.; Dougherty, T. J. Alkyl ether analogs of chlorophyll-a derivatives: Part 1. Synthesis, photophysical properties and photodynamic efficacy. *Photochem. Photobiol.* **1996**, *63,* 194-204.
20. Baron, E. D.; Malbasa, C. L.; Santo-Domingo, D. Fu. P.; Miller, J. D.; Hanneman, K. K.; Hsia, A. H.; Oleinick, N. L.; Colussi, V. C.; Cooper, K. D. Silicon phthalocyanine (Pc 4) photodynamic therapy is a safe modality for cutaneous neoplasms: results of a phase 1 clinical data. *Lasers Surg. Med*. **2010**, *42*, 728-735.
21. Hnderson, B. W.; Bellnier, D. A.; Graco, W. R.; Sharma, A.; Pandey, R. K..; Vaughan, L.; Weishaupt, K. R.; Dougherty, T. J. An *in vivo* quantitative structure activity relationship for a congeneric series of pyropheophorbide derivatives as photosensitizers for photodynamic therapy. *Cancer Res.* **1997**, *57*, 4000-4007.
22. Potter, W. R.; Henderson, B. W.; Bellnier, D. A.; Pandey, R. K.; Vaughan, L. A.; Weishaupt, K. R.; Dougherty, T. J. Parabolic quantitative structure-activity relationships and photodynamic therapy: application of a three-compartment model with clearance to the *in vivo* quantitative structure-activity relationships of a congeneric series of pyropheophorbide derivatives used as photosensitizers for photodynamic therapy. *Photochem. Photobiol.* **1999**, *70,* 781-788.

23. Loewen, G. M.; Pandey, R. K.; Bellnier, D. A.; Henderson, B. W.; Dougherty, T. J. Endobronchial photodynamic therapy of lung cancer. *Lasers Surg. Med*. **2006**, *38*, 364-370.

24. Rigual, S.; Shafirstein, G.; Cooper, M. T.; Baumann, H.; Bellnier, D. A.; Sunar, U.; Rohrbach, D. J.; Wilding, G.; Tan, W.; Sulivan, M.; Henderson, B. W. Photodynamic therapy with 3-(1'-hexyloxyethyl) pyropheophorbide-*a* for cancer of the oral cavity. *Clin. Cancer Res.* **2013**, *19*, 6605-6613.

25. Zheng, G.; Potter, W. R.; Camacho, S. H.; Missert, J. R.; Wang, G.; Bellnier, D. A.; Henderson, B. W.; Rodgers, M. A. J.; Dougherty, T. J.; Pandey, R. K. Synthesis, photophysical properties, tumor uptake and preliminary in vivo photosensitizing efficacy of a homologous series of 3-(1'-hexyloxy)ethyl-3-devinylpurpurin-18-*N*-alkylimides with variable lipophilicity. *J. Med. Chem*. **2001**, *44,* 1540-1559.

26. Kozyrev, A.; Ethirajan, M.; Chen, Y.; Ohkubo, K.; Robinson, B. C.; Brakigia, K. M.; Fukuzumi, S.; Kadish, K. M.; Pandey, R. K. Synthesis, photophysical and electrochemistry of novel near-IR absorbing bacteriochlorins related to bacteriochlorophyll-a. *J. Org. Chem*. **2012,** *77*, 10260-10271.

27. Kozyrev, A. N.; Chen, Y.; Goswami, L. N.; Tabaczynski, W. A.; Pandey, R. K. Characterization of Porphyrins, chlorins, and bacteriochlorins formed via allomerization of bacteriochlorophyll-a. Synthesis of highly stable bacteriopurpurinimides and their metal complexes. *J. Org. Chem.* **2006**, *71*, 1949-1960.

28. Fukuzumi, S.; Ohkubo, K.; Chen, Y.; Pandey R. K.; Zhan R., Shao, J.; Kadish K. M. Photophysical and electrochemical properties of new bacteriochlorins and characterization of radical cation and radical anion species. *J. Phys. Chem. A.* **2002**, *106,* 5106-5113.

29. Basiji, D. A.; Ortyn, W. E.; Lang, L.; Venkatachalam, V.; Morrissey, P. Cellular image analysis and imaging by flow cytometry. *Clin. Lab. Med.* **2007**, *27*, 653-658.

30. Wilson, B. C.; Patterson, M. S. The physics, biophysics, and technology of photodynamic therapy. *Phys. Med. Biol.* **2008**, *53*, 61-109.
31. Wilson, B. C.; Patterson, M. S.; Lilge, L. Implicit and explicit dosimetry in photodynamic therapy: a new paradigm. *Lasers Surg. Med*. **1997**, 12, 182-199.
32. Sunar, U.; Rohrbach, D.; Rigual, N.; Tracy, E.; Keymel, K.; Cooper, M. T.; Baumann, H.; Henderson, B. W. Monitoring photobleaching and hemodynamic responses to HPPH-mediated photodynamic therapy of head and neck cancer: a case report. *Opt. Express.* **2010**, *18*, 14969-14978.
33. Henderson, Barbara W; Baroque C; Tracy, Erin C; Vaughan LA; Loewen, Gregory M; Cooper, Michele T; Baumann, Heinz. Cross-linking of signal transducer and activator of transcription 3--a molecular marker for the photodynamic reaction in cells and tumors. *Clin. Cancer Res.* **2007**, *13*, 3156-3163.
34. Tracy, Erin C; Bowman, Mary Joann; Pandey, Ravindra K; Henderson, Barbara W; Baumann, Heinz. Cell-type selective phototoxicity achieved with chlorophyll-*a* derived photosensitizers in a co-culture system of primary human tumor and normal lung cells. *Photochem. Photobiol.* **2011**, *87*, 1405-1418.
35. Ferrario, A.; von Tiehl, K. F.; Wong, S.; Luna, M.; Gomer, C. J. Cyclooxygenase -2 inhibitor treatment enhances photodynamic therapy-mediated tumor response. *Cancer Res.* **2002,** *62*, 3955-3961.
36. Pandey, R. K.; Bellnier, D. A.; Smith, K. M.; Dougherty, T. J. Chlorin and porphyrin derivatives as potential photosensitizers in photodynamic therapy. *Photochem. Photobiol.* **1991**, *63,* 65-72.
37. PALLAS Program; PALLAS 3.0.10.2 (043003), COMPU DRUG, Chemistry Ltd.
38. Fukuzumi, S.; Ohkubo, K.; Zheng, X.; Chen, Y.; Pandey, R. K.; Zhan, R.; Kadish, K. Metal bacteriochlorins which act as dual singlet oxygen and superoxide generators. *J. Phys. Chem. B*. **2008**, *112*, 2738-2746.

39. Chen, Y.; Potter, W. R.; Missert, J. R.; Morgan, J.; Pandey, R. K. Comparative *in vitro* and *in vivo* studies on long-wavelength photosensitizers derived from bacteriopurpurinimide and bacteriochlorin p_6: Fused imide ring enhances the *in vivo* PDT efficacy. *Bioconjugate Chem.* **2007**, *16,* 1460-1473.

40. Gryshuk, A.; Chen, Y.; Goswami, L. N.; Pandey, S.; Missert, J. R.; Ohulchanskyy, T.; Potter, W.; Prasad, P. N.; Oseroff, A.; Pandey, R. K. Structure-activity relationship among purpurinimides and bacteriopurpurinimides: Trifluoromethyl substituent enhances the photosensitizing efficacy. *J. Med. Chem.* **2007**, *30,* 1754-1767.

41. Srivatsan, A.; Pera, P.; Joshi, P.; Wang, Y.; Missert, J. R.; Tracy, E. C.; Tabaczynski, W. A.; Yao, R.; Sajjad, M.; Baumann, H.; Pandey, R. K. Effect of chirality on cellular uptake, imaging and photodynamic therapy of photosensitizers derived from chlorophyll-a. *Bioorg. Med. Chem.* **2015**, *23*, 3603-3617.